Title
USE OF THE SELF-POTENTIAL METHOD FOR GEOTHERMAL EXPLORATION

Author
Corwin, Robert F.

Publication Date
1975

LBL-3235
UC-11
TID-4500-R62

USE OF THE SELF-POTENTIAL METHOD FOR GEOTHERMAL EXPLORATION

Robert F. Corwin

January 1975

Prepared for the U. S. Energy Research and Development Administration under Contract W-7405-ENG-48

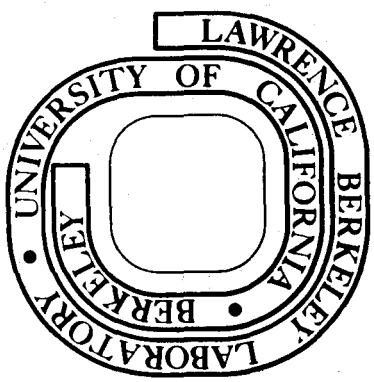

DISCLAIMER

USE OF THE SELF-POTENTIAL METHOD FOR GEOTHERMAL EXPLORATION

Robert F. Corwin[†]

Energy and Environment Division
Lawrence Berkeley Laboratory
Berkeley, CA 94720

ABSTRACT

The applicability of the self-potential method to the location and delineation of geothermal reservoirs is examined. A brief theoretical study indicates that thermoelectric coupling and the motion of subsurface fluid may generate self-potential anomalies. Theoretical and field studies to determine the reproducibility and noise level of self-potential data are described, and the results of self-potential surveys in two geothermal areas of north central Nevada are presented and discussed. It is concluded that observed anomalies of up to 3 km in length and 70 mV in amplitude were due to the motion of subsurface water, and that improvements in equipment and survey procedure could allow observation of self-potential anomalies more directly related to the geothermal reservoir.

[†]Present address: Department of Materials Science and Engineering, University of California, Berkeley, CA 94720.

I. INTRODUCTION

This report is part of a study of the applicability of various geophysical techniques to the location and evaluation of geothermal resources. A small amount of data relating geothermal activity and self-potential has been published (Zohdy and others, 1973; Corwin, 1973; Banwell, 1970), and several personal communications also have indicated that geothermal and self-potential activity may be related. Accordingly, it was decided to carry out self-potential surveys in several areas of known geothermal activity in north central Nevada, in conjunction with the other geophysical methods under evaluation. Preliminary laboratory and field work was conducted in Berkeley and in northern California to evaluate equipment, electrode design, and field procedures.

II. SOURCES OF SELF-POTENTIAL SIGNAL IN GEOTHERMAL AREAS

A geothermal area usually is characterized by the presence of hot, circulating fluid. Both the elevated temperature and the motion of the circulating thermal fluid may contribute to an electric potential field (a self-potential anomaly) generated at the earth's surface.

A. Thermoelectric Coupling

The process by which a subsurface body of elevated temperature may generate an electric potential field at the surface is called thermoelectric coupling. The discussion below is based on the work of Nourbehecht (1963).

The model shown in Figure 1 will be used to obtain a first estimate of the possible thermoelectric field generated by a geothermal source consisting of a sphere of radius 2 km and temperature 150°C (ΔT) above the surroundings. The top of the sphere is 1.7 km below the surface, and intersects a boundary at a depth d of 2 km, resulting in a ratio a/d of 0.5. The electrical conductivity of the lower layer is σ_2 and that of the upper layer is σ_1, and R_{21} is defined as $(\sigma_2 - \sigma_1)/(\sigma_2 + \sigma_1)$. The difference in the theromelectric coupling coefficients of the two layers, $(C_1 - C_2)$, is assumed to be 0.25. The presence of a boundary separating regions of differing thermoelectric coupling coefficients is necessary for the generation of a thermoelectric potential field. A body of elevated temperature buried in a homogeneous half-space will not, according to Nourbehecht, generate a thermoelectric field at the surface.

The potential generated at the surface by a buried sphere as described above is given by the expression

$$f_1(r,o) = (1 + R_{21})(C_1 - C_2)T_o\left(\frac{a}{d}\right) \int_o^\infty \frac{e^{-\xi}}{1 + R_{21}e^{-2\xi}} J_1\left(\frac{a}{d}\xi\right) J_o\left(\frac{r}{d}\xi\right) d\xi \quad ,$$

where

$$f_1(r,o) = \Delta V(r)/[(C_1 - C_2)\Delta T] \quad .$$

Plots of this expression, evaluated for several values of a/d and R_{21}, are shown in Figure 2. For the case described above, where $R_{21} = + 0.5$, the maximum value of $f_1(r,o)$ is about 6 millivolts (mV), decreasing to half this value about 3 km from the center of the anomaly. For a larger (or shallower) source, with (a/d) = 1.0 and a high value of the coupling coefficient difference $(C_2 - C_1)$ of 1.0, the maximum value of the anomaly over the center of the source would be about 60 mV for a conductivity contrast $\sigma_2 = 3\sigma_1$ ($R_{21} = + 0.5$).

Thus, a "typical" thermoelectric self-potential anomaly might be expected to have an amplitude of about 5 or 10 mV, while a very large anomaly would be of the order of several tens of millivolts. The sign of the anomaly would depend on the magnitude of the thermoelectric coupling coefficients of the upper and lower layers. This model obviously is a very crude approximation of a real geothermal reservoir, but should provide at least a reasonable first estimate of the expected magnitude of a thermoelectric anomaly.

B. Streaming Potentials

The motion of subsurface fluid is known to generate electrical fields at the earth's surface. These streaming (or electrokinetic) potentials are due to the Helmholtz double layer which forms at the solid-liquid interface of most geologic materials, and results in preferential binding of ions of one sign to the surface of the solid, with a consequent excess of ions of the opposite sign in the pore fluid. Derivations of analytical expressions for streaming potentials are given by MacInnes (1961, p. 423), Dakhnov (1962, p. 313), and Nourbehecht (1963). For the simple case of a capillary tube containing an ionic fluid (Figure 3), the streaming potential is given by

$$E = \frac{\rho \varepsilon \zeta}{4\pi\eta} \Delta P$$

where E is the streaming potential, ρ is the electrical resistivity of the pore fluid, ε is the dielectric coefficient of the pore fluid, η is the viscosity, ΔP is the pressure difference, and ζ is the "zeta potential", related to the potential between the bound and free ionic layers. (Although the fluid flow rate and the diameter and length of the capillary do not appear in the equation, they are implicit in the pressure difference ΔP).

Thus, motion of underground fluid may constitute a flow of electric charge, equivalent to an ionic current flow, capable of generating an electric field at the earth's surface. Such fields are frequently observed, and in fact constitute a major noise source in self-potential prospecting for ore bodies. However, study of streaming potentials alone has proven useful in gaining a picture of subsurface fluid flow in geothermal and other applications (Bogoslovsky and Oglivy, 1973, 1974; Oglivy and others, 1969; Oglivy, 1970). Due to the great variation of the zeta potential in geologic materials (Oglivy and others, 1969; Nourbehecht, 1963; Tuman, 1963), it is difficult to estimate the streaming potentials to be expected in geologic situations. However, self-potential anomalies of several hundred millivolts, generated by known subsurface fluid flow, have been observed (Poldini, 1938, 1939), and values of 50 - 100 mV are seen often in areas of active subsurface flow, especially over faults along which water is moving. A possible example of a self-potential anomaly caused by ascending geothermal fluid is given by Zohdy and others (1973), and theoretical work by Nourbehecht (1963) indicates that anomalies of several hundred mV may be generated above areas of active flow. Generally, ascending fluid is seen to generate positive anomalies; descending fluid, negative anomalies (Poldini, 1938, 1939). The self-potential anomalies observed in our surveys in north central Nevada probably were due to subsurface water flow (Sections V and VI).

III. DATA ACQUISITION

A. Equipment

The survey equipment used consisted of a digital volt-ohm-milliammeter (DVOM), a light weight reel carrying 500 m of wire, and a pair of copper-copper

sulfate ($Cu-CuSO_4$) electrodes. The DVOM was a Weston model 4440, which had a resolution of 0.1 mV and an input impedance of 50 megohms on the 0 - 199.9 mV range, which was used for all potential readings. The 0 - 20 K ohm resistance scale, which was used to make electrode contact resistance readings for resistances greater than 200 ohms, used a current of 0.1 milliamps (mA), and the 200 ohm range, used for readings of less than 200 ohms, a current of 1.0 mA.

Two types of $Cu-CuSO_4$ electrodes were used, both 3 inches (7.6 cm) in diameter, filled with saturated $CuSO_4$, and having flat porous ceramic bottoms. The first type was fabricated in-house froom Coors No. 71002 "porous pots"; the second was manufactured by the Tinker and Rasor (T & R) Corp. (their model 3A), and had a plastic body and replaceable ceramic junction. Both types seemed to give equal electrochemical performance, but the T & R design was easier to handle in the field. The Coors electrodes were used on lines AA', BB', and EE' in Grass Valley (see Section IV), and the T & R electrodes on lines DD', SP-A, and SP-B in Grass Valley and lines BB' and CC' in Buffalo Valley. The clear plastic window in the body of the T & R electrode allowed instant and continuous observation of the $CuSO_4$ level without the necessity of opening the electrode, but it was observed that sunlight shining in the windows had a photoelectric effect; the sunlit electrode becoming as much as 1 mV positive relative to the shaded one. For this reason an effort was made to keep the windows of the T & R electrodes in the shade when reading.

B. Electrode Response To Chemical Changes

The background noise level in self-potential surveys usually is about ±5 to ±10 mV (Parasnis, 1966, p. 76) with differences of 5 to 10 mV often seen between points only a few cm apart (Figure 4). Many factors, including streaming potentials and local changes in the temperature, moisture content, and chemistry of the soil contribute to this noise. Of particular interest in geothermal areas are changes in soil chemistry, as the soil in such areas often contains salts or saline solutions whose composition or concentration may vary widely from point to point.

A crude field experiment was run to check electrode response to variation of soil properties. Soil samples were taken from around and directly below the electrode holes at two stations 100 m apart. The soils were placed in contact in a plastic container and the potential between the soil samples mea-

sured with Cu-$CuSO_4$ electrodes. This experiment was repeated several times, and often a potential similar to that seen between the field stations was observed between the isolated soil samples. Although the experiment was not well controlled, and the results were not very consistent, they did indicate that a "soil cell", isolated from the environment, can generate electrode potentials. Ewing (1939) found potential differences of up to 6 mV to be generated by similar soil cells.

A brief theoretical and laboratory experiment was carried out to determine the magnitude of the potentials which might be generated by changes in soil chemistry. The situation studied is shown in Figure 5. The soil water is assumed to contain ions in concentrations C_1', C_2', . . . C_n' on one side of a permeable boundary, and the same ions in concentrations C_1'', C_2'', . . . C_n'' on the other side. The potential V appearing across a voltmeter will be the sum of five potentials: E_1 and E_5, the potential between the copper rod and the $CuSO_4$ electrolyte; E_2 and E_4, the liquid junction potential between the $CuSO_4$ and the soil water; and E_3, the liquid junction potential between the two soil water solutions.

Assuming that both electrodes contain pure $CuSO_4$ electrolyte at the same (saturated) concentration and temperature, E_1 will equal $-E_5$, and V will just be $E_2 + E_3 + E_4$. These liquid junction potentials may be estimated by use of the Henderson equation (MacInnes, 1961, p. 232; Ives and Janz, 1961, p. 54; Dakhnov, 1962, p. 291):

$$E_L = \frac{RT}{F} \frac{\Sigma_n \frac{U_i}{Z_i}(C_i'' - C_i')}{\Sigma_n U_i(C_i'' - C_i')} \ln \frac{\Sigma_n C_i' U_i}{\Sigma_n C_i'' U_i} ,$$

where E_L = liquid junction potential, volts
R = universal gas constant, 8.315 joules/°K
T = absolute temperature, °K
F = Faraday's constant, 96500 coulombs/mole
U_i = mobility of ion i, cm^2/sec volt
Z_i = valence of ion i (with appropriate sign)
C_i = concentration of ion i, equivalents/liter.

The cell

$$\underset{E_1}{Cu,\ CuSO_4} : \underset{E_2}{NaCl\ (C')} : \underset{E_3}{NaCl\ (C'')} : \underset{E_4}{CuSO_4} , \underset{E_5}{Cu}$$

was used as a test case to check the magnitude of the potentials generated by groundwater chemistry concentration cells (the colon indicates a liquid junction). The calculation of $V(= E_2 + E_3 + E_4)$ for C' = 1M and C'' = 0.1, 0.01 and 0.001 M is shown in the Appendix, and the results plotted in Figure 6. Also shown on Figure 6 are experimental values obtained to check the calculated results. Both the theoretical and laboratory work indicate a slope of about -6 mV/decade concentration change. The laboratory result diverges from the theoretical one at a concentration ratio of 1000:1, probably because the 0.001 M solution became contaminated by leakage of 1 M solution through the porous membrane, and by Cu^{++} and SO_4^{+} ions from the electrode. However, the results indicate that Cu-$CuSO_4$ electrodes do respond to changes in soil water chemistry, and that these changes are of similar magnitude to those observed as short-wavelength geological noise on self-potential data. More work is needed on this subject, especially on determination of point-to-point variations of actual soil moisture chemistry.

C. Field Procedure and Data Reproducibility

The ease with which self-potential data is obtained is balanced by the difficulty of reproducing the data in subsequent surveys. Two main factors contribute to this difficulty: electrode effects and telluric currents.

1. Electrode effects

Changes in moisture content, temperature, and chemical composition of the soil affect the potential between the electrodes. As a finite time is required for an electrode to respond to these changes, such changes also cause drift. Electrodes often become significantly polarized when inserted into environments of varying chemistry, probably due to absorption of contaminating ions by the ceramic junction of the electrode. For the field surveys described below,

electrode polarization was measured after each tie-in reading by setting both reference and scanning electrodes on a sponge saturated with saturated $CuSO_4$. Polarization generally was less than 3 mV, but larger readings of 5 or 6 mV were sometimes seen, and once (after use in very moist and salty soil), the value was 11 mV.

These large polarizations were compensated by adjusting the reading at the tie-in point. This method is arbitrary, as it is not known when the polarization actually took place, but at least helps to reduce the cumulative error at tie-in points. When the electrodes were allowed to remain at open circuit on the sponge, this usually resulted in their returning to normal polarization levels within 10 or 15 minutes to one hour, presumably because the contaminating ions were diluted and flushed out by the excess $CuSO_4$ on the sponge.

Removal and re-insertion of an electrode usually results in a change of one or two mV in the reading, if the electrode hole is not disturbed. This change probably is due to the small amount of drying of the soil moisture and $CuSO_4$ in the soil, and to the slight change in contact position of the electrode.

The contact resistance between the electrodes was found to significantly affect the self-potential readings, especially in the very dry soil found in many parts of the desert; the resistance between a pair of electrodes in saturated $CuSO_4$ liquid was about 75 ohms. As the voltmeter used in the survey had an input impedance of 50 megohms, it would be expected to give accurate readings as long as the resistance between the electrodes was kept below about 50 kilohms. It was found, however, that when contact resistance read above about 20 kilohms, the potential readings drifted badly and showed a large, erratic change (of the order of 10 mV) when the electrode was reseated. If contact resistances were kept below 20 kilohms, the potentials showed much smaller (a few mV), but still erratic, changes with contact resistance.

The standard method of reducing the contact resistance of "non-polarizing" electrodes is to install them in a hole which has been liberally soaked with water. This procedure is not advisable for self-potential surveys, as it was found that wetting an electrode caused it to become about 10 mV positive with respect to the dry electrode, with a subsequent large drift. If both electrodes are wetted at the same time, the potential between them will change with unpredictable magnitude and sign. For this reason, the electrodes used in these surveys were not wetted. Instead, they were inserted in holes dug deeply enough

to encounter sufficient soil moisture to allow a reasonable contact resistance. This procedure also resulted in more uniform electrode temperatures. As the potential between a pair of $CuSO_4$ electrodes varies about 1/2 mV per °C (Ewing, 1939), this is an important consideration. Every effort was made to keep the contact resistances as uniform as possible from hole to hole, even when this required the excavation of pits 1/2 m deep in very soft or rocky soil and great care in preparing a seating surface for the electrode. Although this procedure was slow and tedious, it was deemed necessary to ensure reproducible results.

The reproducibility of self-potential data also is affected by drift of the readings. Usually, a reading will drift one or two mV negative in the first few seconds after installing the scanning electrode, then continue to drift negative at a decreasing rate. This drift presumably is caused by diffusion of $CuSO_4$ out of the scanning electrode, as the polarity of the drift reverses if the reference electrode is removed and re-installed. For our field readings, an initial reading was taken within a few seconds of emplacing the scanning electrode. Then, the contact resistance was measured as quickly as possible to minimize electrode polarization, and the reading allowed to drift to a "final" value. The "jolt" to the electrodes caused by the resistance measurement usually lasted a few seconds, and the reading generally would reach a reasonably stable value, one or two mV more negative than the initial reading, in less than one minute. The reading was considered stable when the drift rate (exclusive of tellurics, see below) was less than about 0.1 mV in 20 seconds.

Occasionally, much greater drift would be encountered. This severe drift was almost always negative, and could continue for 5 or 10 minutes before stabilizing. Sometimes the electrodes were found to be polarized badly after a series of such readings, but this was not always the case. Also, very rarely, the drift would be positive from the initial reading rather than negative. Possibly these two "abnormal" drift patterns were caused by some chemical condition in the soil or by clogging or leakage of the electrode, although none of these conditions were apparent at the time.

2. Tellurics

Telluric currents with periods longer than about one second decrease the reproducibility of self-potential data. While most long-period telluric activity is in the 10 to 40 second range, there may be significant energy at much longer

periods (Keller and Frischknecht, 1966, p. 205). Telluric potentials with periods between 10 and 40 seconds observed in Nevada ranged from undetectable to as much as about ±7 or 8 mV were a nuisance in that readings had to be taken for several minutes, and successive highs and lows averaged to calculate the "true" reading. As the telluric signals were far from regular or uniform, this averaging process was a definite source of error.

Tellurics with periods greater than 2 or 3 minutes could be even a greater source of error, as they might not be recognized during our reading interval. In order to check the magnitude of these long-period tellurics, an orthogonal pair of 300 m dipoles was set up at the location indicated on Figure 13, and the output monitored for a 24 hour period on a pair of chart recorders. The arrangement of the monitoring system is shown in Figure 7, and the output of the chart recorders is shown in Figure 8. As independent pairs of electrodes were used for each dipole, any event appearing simultaneously on both records probably represents an external signal rather than an electrode effect, although both electrodes may show similar simultaneous drift due to diurnal changes in ground temperature. A possible long-period telluric event may be seen on both records between about 1400 and 2000. The signal has an absolute amplitude of about 13 mV per km and could cause a difference of about 6 mV in readings taken between two points 500 m apart at, say, 1500 and 1730. The general negative trend seen on the records probably is due to electrode drift, but may be caused by tellurics with periods of many hours or even days. Such long-period events could seriously affect day-to-day reproducibility of self-potential readings.

3. Combined errors

The electrode effects and tellurics discussed above contribute to an uncertainty in each self-potential reading. If successive surveys are made using the same holes on a given line on the same day, under good conditions (moist soil and low, uniform contact resistance), the average uncertainty of any reading is about ±2 mV, with a maximum error of about 10 mV (see Figures 9 and 10). Under poor conditions (very dry and/or rocky soil, as often found in the desert), similar results are obtained if care is taken to minimize contact resistance. The results of two desert surveys, run 5 weeks apart and using hole locations at least 1 m apart are shown in Figure 11.

The importance of the errors described above depends on the demands of the survey. In self-potential surveys for sulfide ore bodies, where anomaly amplitudes are commonly greater than 100 mV and anomaly widths usually less than 1 km, these errors would not be highly significant. However, in searching for a possible anomaly produced by thermoelectric coupling (Section II A), with an amplitude of 10 mV and a wavelength of several km, such errors could swamp the anomaly. These errors are especially significant at tie-in points, where the reference electrode is advanced to the last previous survey point. For this reason, it is desirable to minimize the number of tie-ins required. The accumulation of tie-in errors would preclude use of the "gradient" method of surveying (Edge and Laby, 1931; Parasnis, 1966), in which a dipole of fixed length is moved along the survey line, when long-wavelength, low-amplitude anomalies are sought.

It is desirable, then, to use the greatest possible wire lengths for geothermal self-potential surveys. Unfortunately, as telluric signals increase linearly with dipole length, readings become more difficult at increasing wire length. Nevertheless, it appears that tie-ins should be limited to a maximum of 2 or 3 per survey line to minimize cumulative errors. Logistic problems limited us to a reel holding 500 m of wire, necessitating tie-ins at 500 or 1000 m intervals. The result of systematic, cumulative error (of unknown origin), may be seen on Figure 20. The symmetrical, concave shape of the curve (run with 500 m tie-ins) was not seen in two later surveys on the same line, one using 100 m tie-ins (Figure 21) and the other "leap-frogging" electrodes at 500 m intervals.

In summary, with the equipment and procedures used for these surveys, anomalies with lengths of less than 2 or 3 km and amplitudes greater than about 15 mV probably are real, while those of greater length or lower amplitude are suspect. The estimated reliability of the data for each survey line is discussed in Section IV, and suggestions for improving data reliability are given in Section V.

IV. SELF-POTENTIAL SURVEY RESULTS

During the period from late August through early October, 1974, 71 line kilometers of self-potential survey were run in geothermal areas of north central Nevada; 43 km at Grass Valley, south of Winnemucca; and 28 km at Buffalo Valley,

south of Battle Mountain (Figure 12). The survey lines are shown in Figures 13 and 14, and the data along each of the lines is discussed below.

A. Grass Valley

1. Lines AA', SP-A, SP-B, and EE'

The data from line AA' is shown in Figure 15. The features of greatest interest on this line are the positive anomaly over Leach hot springs (centered at 3.25 km north) and the large negative anomaly centered at 3.55 km north. It is not certain that the generally downward slope of the data from north to south between 1.5 km south and 2 km north and between 5.5 km north and 8 km north is real, as these lines were not re-run. The positive "bump" between 2 and 3 km north may be related to the isolated warm spring, about 0.5 km west of line AA', shown on Figure 13.

The positive anomaly over the hot springs is difficult to distinguish from the background noise, but a comparison with the data from line SP-A (Figure 16) seems to show the same anomaly in the same position. The center of the large negative anomaly is north of a well-defined fault scarp running through the hot springs (hereafter called the hot springs fault) on line AA'. However, on line SP-A, the center of the same anomaly appears to the south of the hot springs fault scarp. The shapes of the negative anomalies on lines AA' and SP-A are remarkably similar.

The data from line EE' is shown in Figure 17. The negative anomaly related to the hot springs fault system is again seen, reduced in amplitude and centered at 900 m southeast (just northwest of the hot springs fault scarp). Other negative anomalies, centered at 1.6, 3.0, and 3.7 km southeast, appear to be related to mapped faults. It is not certain that the general positive trend of the data to the southeast and northwest of 1.0 km southeast is real. A short line, SP-B, run parallel to and about 250 m north of EE', shows only a vague remnant of the negative anomaly (Figure 18).

The data from lines AA', SP-A, EE', and SP-B has been contoured (Figure 19). These contours must be considered only as rough estimates, due to the high geologic noise level and the short length of lines SP-A and SP-B. Also shown on Figure 19 are fault traces and water table levels (the water table information was obtained from F.H. Olmsted, U.S. Geological Survey, Menlo Park,

by written and verbal communication, 1974). It appears that the self-potential contours are closely related to the flow of subsurface water around the hot springs fault system. The sharp positive "ridge" through the hot springs probably is related to the upward flow of thermal water to the springs. It is interesting that this "ridge" extends from the hot springs at least to line SP-A, possibly also appearing on line EE'. This positive area may indicate an upward flow of thermal water which does not appear at the surface. As a similar positive self-potential anomaly also is seen over the hot springs in Buffalo Valley (discussed below), and over the geothermal area in Yellowstone National Park (Zohdy and others, 1973), it seems reasonable to conclude that positive self-potential anomalies are related to ascending fluid, and that negative anomalies indicate descending fluid. The most striking feature of the self-potential contours of Figure 19 is the strong negative anomaly centered about 1/2 km north of the hot springs and running northwest-southeast. This anomaly would seem to indicate an intense downward flow of subsurface water along a zone almost perpendicular to the two major faults, parallel to the rising thermal water. Unfortunately, there is not enough drill hole data to establish whether this is nonthermal water "dammed" by the fault system, thermal water which does not emerge at the surface, or a mixture of the two. Additional drill holes would be helpful in resolving this question.

2. Line BB' (and systematic error on other lines)

The data from line BB' is shown in Figure 20. As mentioned previously, the overall concave shape of the curve is not real, as it vanished when the line was re-run (Figure 21). This shape, also seen on line EE', probably is due to some systematic error in the field procedure, but the source of the error is not apparent. Surveys on lines AA' and EE', and the initial survey on BB', were run with tie-ins every 500 m, using the Coors electrodes. On line EE', the survey was run northwest and southeast from a zero point at 500 m northwest. Therefore, on line EE', with the exception of the large anomaly at the hot springs fault scarp, the data trends positive in the direction the scanning electrode is advancing. However, the survey on BB' was run continuously to the west from a zero point at 4 km east, and the data is seen to trend negative and then positive in the direction of advance. Line AA' was surveyed north

and south from the 0 km point, and no consistent correlation with direction of advance is seen.

It is apparent from Figure 21 that most of the point-to-point variations of the data are repeatable, even though the surveys were run 6 weeks apart, and a separation of at least 2 m was maintained between old and new electrode locations at each station. Therefore, small-scale anomalies such as those centered at about 1.8 km east and at 0 km are probably real, and may represent subsurface water circulation or local soil chemistry changes. The small negative anomaly, centered over the fault zone at about 900 m east, is of doubtful significance.

3. Line DD'

The data from line DD' is shown in Figure 22. The field procedure was changed somewhat from that used on lines AA', BB', and EE' in that the T & R electrodes were used, and the survey was run by moving the reference electrode forward 1000 m at a time, then surveying back and forward 500 m, thus reducing the number of tie-ins and the time required to pack the equipment and move the reference electrode. Of interest are the large, sharp anomalies at the extreme east and west ends of the survey line. These probably are related to water flow along faults which showed prominent surface scarps. Vegetation changes at about 2500 and 3800 m east are reflected in the self-potential data, and may be due to changes in water flow and/or soil chemistry.

B. Buffalo Valley

The survey lines in Buffalo Valley are shown in Figure 14.

1. Line BB'

The data from line BB' is shown in Figure 23. Starting at about 5 km, this line shows a good deal of "character". Interestingly, no anomaly is seen at the point of closest approach to the hot springs at 8.2 km west. The positive anomaly centered at 11 km probably is real, and may indicate ascending subsurface water. The anomaly centered at about 15.5 km may indicate downward

flow of water through a fault zone. The general trend of the data upward to the west may be due to a general downward movement of groundwater from west to east, or to cumulative measuring error. As on line CC' (below), the presence of salt on the soil surface did not seem to directly affect the self-potential readings. The salt crust was removed, exposing the bare, moist, salty soil beneath before emplacing the electrode.

2. Line CC'

The data from line CC' is shown in Figure 24. Of interest is the positive anomaly over the Buffalo Valley hot spring area, centered at about 4.2 km, which probably is related to ascending thermal water. The anomaly is broader and lower in amplitude than that seen over Leach hot springs, reflecting the greater lateral extent and lower water flow of Buffalo Valley hot springs. The positive trend from 5.5 to 8.5 km probably is real, and may be related to the positive anomaly centered at 11 km on line BB'. Unfortunately, not enough drillhole data is available yet in Buffalo Valley to compare self-potential and water table information.

V. CONCLUSIONS AND RECOMMENDATIONS

The brief theoretical and field results presented in this report indicate that detectable self-potential anomalies are generated by geothermal activity. Some conclusions and recommendations regarding survey procedure, data interpretation, and future work are given below.

A. Data Acquisition

1. Electrodes

As discussed in Section III A, electrode response to changes in soil chemistry and moisture content appears to be a major source of irreproducibility and background noise in self-potential surveys. Further research in this area could help to improve data accuracy and precision. Specific projects should include studies of soil moisture content and chemistry in geothermal areas,

and expansion of the theoretical and laboratory studies of electrode response to chemical changes described in Section III B. Also, studies of improved electrode designs and implantation procedures would be of value. For example, it was seen that insertion of a $CuSo_4$-saturated sponge in the hole before emplacing the electrode helps to reduce contact resistance, and if a fresh sponge is used for each hole, should reduce electrode polarization by preventing contaminating ions from reaching the porous ceramic junction. Silver-silver chloride electrodes are known to have lower temperature response than the Cu-$CuSO_4$ type, and also may have better electrochemical characteristics. Or, it may prove desirable to collect soil samples for each survey point and to correct the field data according to the local soil chemistry.

2. Survey procedure

As discussed in Section III C, the survey procedure used strongly affects the reproducibility of the data. Specifically, if long-wavelength low-amplitude anomalies are sought, the number of tie-in points must be reduced (ideally, tie-ins should be eliminated, and a single reference point used for the entire survey). This would suggest the use of lightweight, disposable wire, which could be left on the ground after use, and picked up only after completion of the entire survey. As this arrangement would require very large electrode separations, it would be desireable to continuously record tellurics, at a central location, for later correction of the data. Another possibility would be to reverse the sign of a reference telluric signal and feed it back, with appropriate amplification, into the self-potential recording instrument, thus cancelling the telluric variations. To check survey electrode polarization, it would be desireable to use at least two electrodes in each survey hole, one after the other, and to check each of these against a third, reference electrode set on an electrolyte-saturated sponge. Finally, it might be useful to feed the self-potential signal into a chart recorder as well as the high-impedance digital voltmeter, to record drift and tellurics.

The procedures described above would decrease the speed and increase the cost of the self-potential survey. It would be worthwhile, however, to try such a survey at least once, preferably in a geothermal area where the geology and hydrology are well known.

B. Data Interpretation

1. Field data

The field data was discussed in Section IV. It appears that the observed self-potential anomalies were generated by the motion of subsurface water, with positive anomalies caused by ascending water, and negative anomalies by descending water. Because of the field techniques used, the only anomalies considered real were steep-sided and had lengths not exceeding about 3 km. Therefore, no attempt was made to analyze the data for information about deepseated geothermal sources. Such information may be contained in the data, which should be re-examined when the results of geological and other geophysical surveys become available.

2. Theoretical studies

Some possible mechanisms by which self-potential anomalies may be generated by geothermal activity were discussed briefly in Section II. Little work has been done in this area. More data is needed on thermoelectric coupling coefficients and zeta potentials, especially for thermal water flowing in hydrothermal environments. Such data, combined with reasonable assumptions about the shape, temperature, and hydrology of geothermal reservoirs, should allow analytical models to be set up to calculate self-potential anomalies generated by thermoelectric coupling and streaming potentials.

VI. ACKNOWLEDGEMENTS

I would like to thank Professor H.F. Morrison, University of California, Berkeley, for his assistance with this work; Birendra Jain, for his help in the laboratory and field work and computer programming; and Rida Bakbak, Mark Chang, Gail Mahood, Alfred Liaw, E.O. Davisson, and Harold Meyer for their assistance with the field work and their many valuable suggestions.

This work was performed in part in facilities provided by the U.S. Atomic Energy Commission

VIII. REFERENCES

Banwell, C.J., 1970, Geophysical Techniques in Geothermal Exploration, in United Nations Symposium on the Development and Utilization of Geothermal Resources, Pisa, Italy.

Bogoslovsky, V.V., and Oglivy, A.A., 1973, Deformations of Natural Electric Fields Near Drainage Structures: Geophysical Prospecting, v. 21, no. 4, p. 716 - 723.

Bogoslovsky, V.A., and Oglivy, A.A., 1974, Detailed Electrometric and Thermometric Observations in Offshore Areas: Geophysical Prospecting, v. 22, no. 3, p. 381 - 392.

Corwin, R.F., 1973, Offshore Application of Self-Potential Prospecting: Ph.D. Thesis, University of California, Berkeley, 303 p.

Dakhnov, V.N., 1962, Geophysical Well Logging: Quarterly of the Colorado School of Mines, v. 57, no. 2, 445 p.

Edge, A.B., and Laby, T.H., 1931, The Principles and Practice of Geophysical Prospecting: Cambridge University Press, London, 372 p.

Ewing, S., 1939, The Copper-Copper Sulfate Half-Cell for Measuring Potentials in the Earth: Technical Section, American Gas Association Distribution Conferences, 1939.

Getman, F.H., and Daniels, F., 1931, Outlines of Theoretical Chemistry (5th ed.): Wiley, New York, 643 p.

Ives, D.J.G., and Janz, G.J., 1961, Reference Electrodes -- Theory and Practice: Academic Press, London, 651 p.

Keller, G.V., and Frischknecht, F.C., 1966, Electrical Methods in Geophysical Prospecting: Pergamon Press, Oxford, 519 p.

Lange, N.A., ed., 1963, Handbook of Chemistry: McGraw-Hill, New York, 2001 p.

MacInnes, D.A., 1961, The Principles of Electrochemistry: Dover, New York, 478 p.

Moore, W.J., 1962, Physical Chemistry (3rd ed.): Prentice-Hall, Englewood Cliffs, New Jersey, 845 + XXV p.

Nourbehecht, B., 1963, Irreversible Thermodynamic Effects in Homogeneous Media and Their Applications in Certain Geoelectric Problems: Ph.D. Thesis, Massachusetts Institute of Technology, Cambridge, 121 p.

Oglivy, A.A., Ayed, A.A., and Bogoslovsky, V.A., 1969, Geophysical Studies of Water Leakages from Reservoirs: Geophysical Prospecting, v. 27, no. 1, p. 36 - 62.

Ogilvy, A.A., 1970, Geophysical Proespecting for Groundwater in the Soviet Union, in Mining and Groundwater Geophysics/1967, Morley, L.W., ed.: Geological Survey of Canada, Ottawa, Economic Geology Report no. 26, p. 536 - 543.

Parasnis, E.S., 1966, Mining Geophysics: Elsevier, New York, 356 p.

Poldini, E., 1938, 1939, Geophysical Exploration by Spontaneous Polarization Methods: The Mining Magazine, v. 59, p. 278 - 282, p. 347 - 352; v. 60, p. 22 - 27, p. 90 - 94.

Prutton, C.F., and Maron, S.H., 1944, Fundamental Principles of Physical Chemistry: MacMillan, New York.

Robinson, R.A., and Stokes, R.H., 1959, Electrolyte Solutions: Academic Press, New York, 559 p.

Tuman, V.S., 1963, Thermo-Telluric Currents Generated by an Underground Explosion and Other Geologic Phenomena: Geophysics, v. 28, no. 1, p. 91 - 98.

Zohdy, A.A.R., Anderson, L.A., and Muffler, L.J.P., 1973, Resistivity, Self-Potential, and Induced-Polarization Surveys of a Vapor-Dominated Geothermal System: Geophysics, v. 38, no. 6, p. 1130 - 1144.

IX. APPENDIX

CALCULATION OF LIQUID JUNCTION POTENTIALS

For the electrochemical cell

$$\underset{E_1}{Cu,\ CuSO_4(sat.)} : \underset{E_2}{NaCl\ (C')} : \underset{E_3}{NaCl\ (C'')} : \underset{E_4}{CuSO_4(sat.)} , \underset{E_5}{Cu}$$

the total potential V appearing across the electrodes is the sum of the liquid junction potentials $E_2 + E_3 + E_4$, as $E_1 = -E_5$ (the colon denotes a liquid junction). For this example, C' = 1 M and C'' = 0.1, 0.01, and 0.001 M, and the temperature = 25°C.

1. Calculation of E_3

If the solutions on either side of a liquid junction are the same univalent salt at different concentrations C' and C'', the Henderson equation simplifies to

$$E_L = (2t^+ - 1)\frac{RT}{F}\ln\frac{C'}{C''} \qquad (1)$$

where t^+ is the transference number of the positive ion (MacInnes, 1961, p. 232). For Na^+, $t^+ = 0.39$, and remains reasonably constant with varying concentration (ibid., p. 226). Then, for T = 25°C (298.1°K),

$$E_3 = \frac{[2(0.39) - 1](8.315)(298.1)}{96500}\ln\frac{C'}{C''}\ \text{(volts)} \quad . \qquad (2)$$

The values of E_3, for C' = 1M and varying C'' are given in the table below.

TABLE 1.

C'' (M)	0.1	0.01	0.001
E_3 (mV)	-13	-26	-39

2. Calculation of E_2 and E_4

As different ions, some of which are divalent, are present on the two sides of these junctions, the full Henderson equation

$$E_L = \frac{RT}{F} \frac{\sum_n \frac{U_i}{Z_i} (C_i'' - C_i')}{\sum_n U_i (C_i'' - C_i')} \ln \frac{\sum_n C_i' U_i}{\sum_n C_i'' U_i} \quad (3)$$

must be used. Therefore, values for U_i, the mobilities of each ion, must be known for the concentrations used. Mobilities appear to be listed in the literature only for solutions at infinite dilution. For example, Moore (1962), p. 337 gives:

TABLE 2.

ion	Na^+	Cl^-	$SO_4^=$
U, $cm^2\ sec^{-1}\ volt^{-1}$ (25°C)	5.19×10^{-4}	7.19×10^{-4}	8.27×10^{-4}

For non-zero concentrations, mobilities may be calculated from

$$U = \frac{t\lambda}{F} \quad (4)$$

(Moore, 1962, p. 334), where λ is the equivalent conductivity of the solution:

$$\lambda = \frac{1000\ \sigma}{C_{eq}} \quad (5)$$

where σ = specific conductivity ($ohm^{-1}\ cm^{-1}$) and C_{eq} = concentration in equivalents per liter (Moore, 1962, p. 328). Therefore, if λ and t are known as a function of concentration, the ion mobilities may be calculated.

A. Values of λ, t, and U for NaCl

From Robinson and Stokes (1959), p. 466, for 25°C, the table below lists corresponding values of NaCl concentration and equivalent conductivity.

TABLE 3.

C (moles/liter)	λ (cm^2 ohm^{-1} $equiv^{-1}$)
0	126.45
0.0005	124.51
0.001	123.74
0.005	120.64
0.01	118.53
0.05	111.06
0.1	106.74
0.5	93.62
1.0	85.76

For the junction $CuSO_4$: NaCl (1M), C_{NaCl} = 0 on the left side and 1M on the right side, so the average concentration is 0.5M and λ = 93.62. As mentioned above, t^+_{Na} for NaCl is reasonably constant at 0.39.
As

$$t^+ + t^- = 1 \qquad (6)$$

(MacInnes, 1961, p. 60), t^-_{Cl} = (1 - 0.39) or 0.61. Substituting these values in (4), $U^+_{Na} = 3.78 \times 10^{-4}$, and $U^-_{Cl} = 5.92 \times 10^{-4}$ cm^2 sec^{-1} $volt^{-1}$. Using similar reasoning for C_{NaCl} = 0.1, 0.01, and 0.001, the values tabulated below may be calculated:

TABLE 4.

C_{NaCl}	1.0	0.1	0.01	0.001
$C_{average}$	0.5	0.05	0.005	0.0005
U^+_{Na}, cm^2 sec^{-1} $volt^{-1}$	3.78×10^{-4}	4.49×10^{-4}	4.88×10^{-4}	5.03×10^{-4}
U^-_{Cl}, cm^2 sec^{-1} $volt^{-1}$	5.92×10^{-4}	7.02×10^{-4}	7.63×10^{-4}	7.87×10^{-4}

B. Values of λ, t, and U for $CuSO_4$

The molecular weight of $CuSO_4$ is 159.6. At 25° C, a saturated $CuSO_4$ solution contains 228.5 g/liter, or 1.43M (Lange, 1967, p. 1098). As the valance of Cu^{++} and $SO_4^{=}$ is 2, C_{eq} = 1.43/2 or 0.715 equivalents/liter. However, as the concentration of $CuSO_4$ is 0 in the NaCl solution, an average concentration of 0.715/2, or 0.36 equiv/liter, will be used. From Moore (1962), p. 329, λ = 48 cm^2 ohm^{-1} $equiv^{-1}$ at C_{eq} = 0.36 equiv/liter, at 18°C. This may be corrected to 25°C by using an equation given by Getman and Daniels (1931, p. 387). For $CuSO_4$,

$$\frac{1}{\lambda}\frac{\Delta\lambda}{\Delta T} = 0.0225 \qquad (7)$$

where ΔT is the temperature change, in °C. For the case above,

$$\Delta\lambda = (0.0225)(48)(25 - 18) = 8$$

so λ_{CuSO_4} at 25°C = (48 + 8) or 56 cm^2 ohm^{-1} $equiv^{-1}$.

From Prutton and Maron (1944), p. 440, at 18°C, t^+_{Cu} in $CuSO_4$ is 0.361 at C_{eq} = 0.2 and 0.327 at C_{eq} = 0.5, so, by interpolation, for C_{eq} = 0.36, $t^+_{Cu_{25°}}$ = 0.34. Correcting to 25°C by using

$$t^+_{Cu_{25°}} = 0.34 \times \frac{\lambda_{25°}}{\lambda_{18°}} = 0.34 \times \frac{56}{48} = 0.40 \quad ,$$

t^+_{Cu} for $CuSO_4$ is 0.40 and $t^-_{SO_4}$ is (1 - 0.40) = 0.60. Then, from (4), U^+_{Cu} = 2.32×10^{-4} and $U^-_{SO_4}$ = 3.48×10^{-4} cm^2 ohm^{-1} $equiv^{-1}$.

C. Calculation of Junction Potentials

The information derived in Sections A and B above is summarized in the table below:

TABLE 5.

i	ion	Z_i	C_i =	$U_i \times 10^{-4}$			
				1	0.1	0.01	0.001
1	Na^+	+1		3.78	4.49	4.88	5.03
2	Cl^-	-1		5.92	7.02	7.63	7.87
3	Cu^{++}	+2		2.32	2.32	2.32	2.32
4	$SO_4^=$	-2		3.48	3.48	3.48	3.48

For T = 25°C, the constant RT/F = 0.02343. Substituting this and the above values into the Henderson equation (3), the results tabulated below are obtained. Also listed below are the laboratory results discussed in Section III B.

TABLE 6.

C''_{NaCl}	0.1	0.01	0.001
E_2 (mV)	+ 6	+ 6	+ 6
E_3 (mV)	-13	-26	-39
E_4 (mV)	+ 2	+ 8	+14
V calculated (mV)	- 5	-12	-19
V measured (mV)	- 4	-13	-14

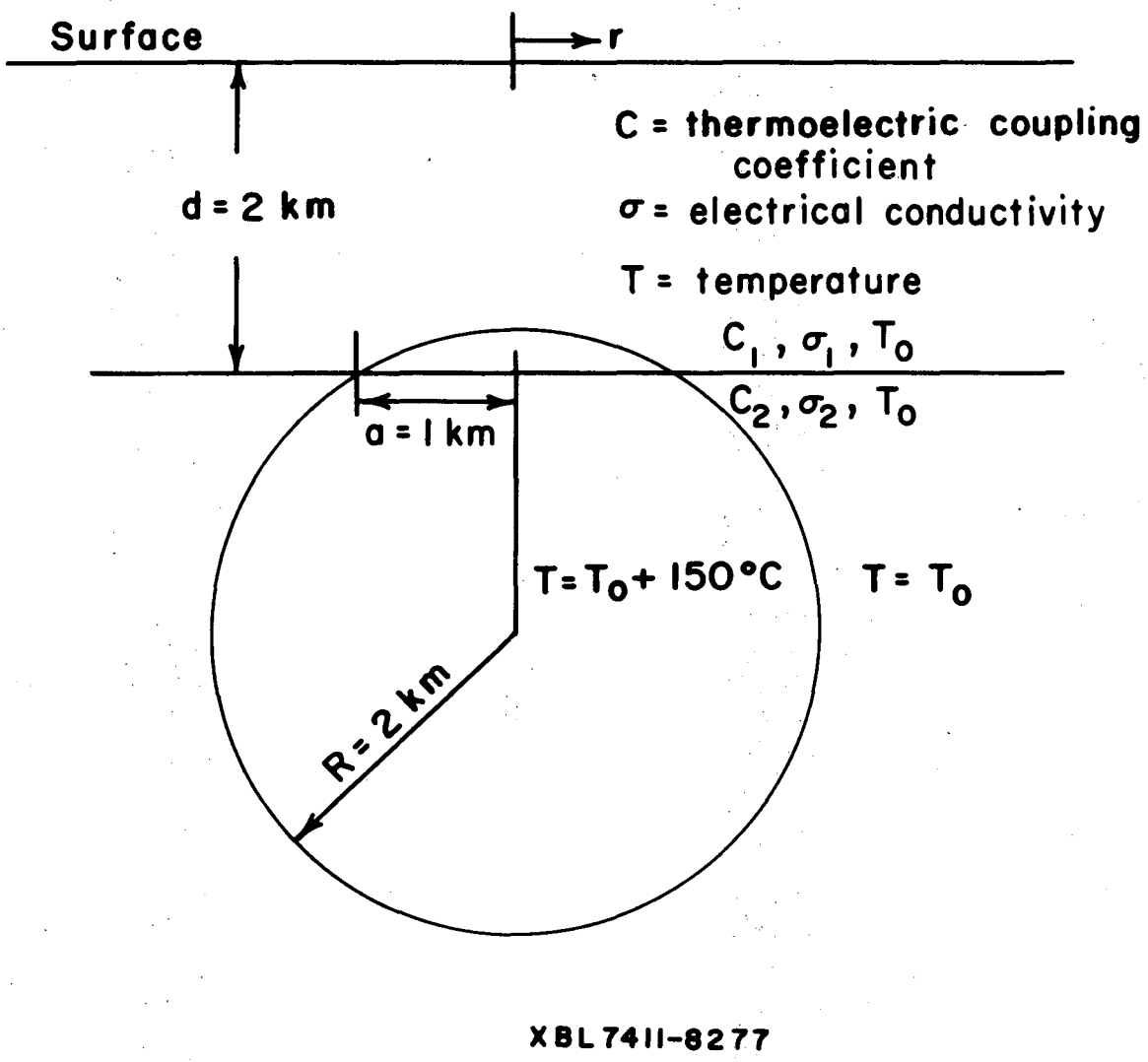

Fig. 1. Thermoelectric Potential Generation (After Nourbehecht, 1963).

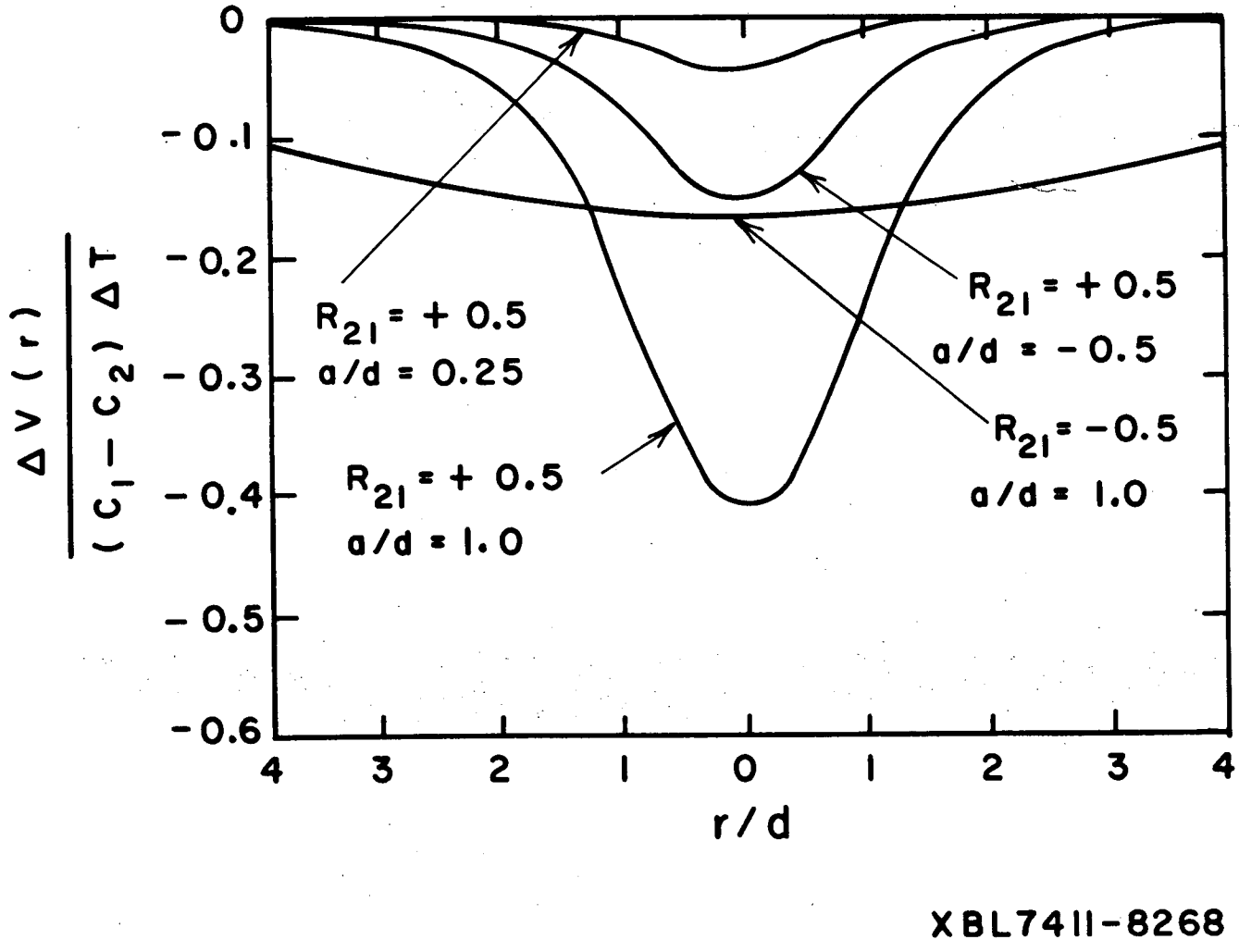

Fig. 2. Plots of Thermoelectric Potential (After Nourbehecht, 1963).

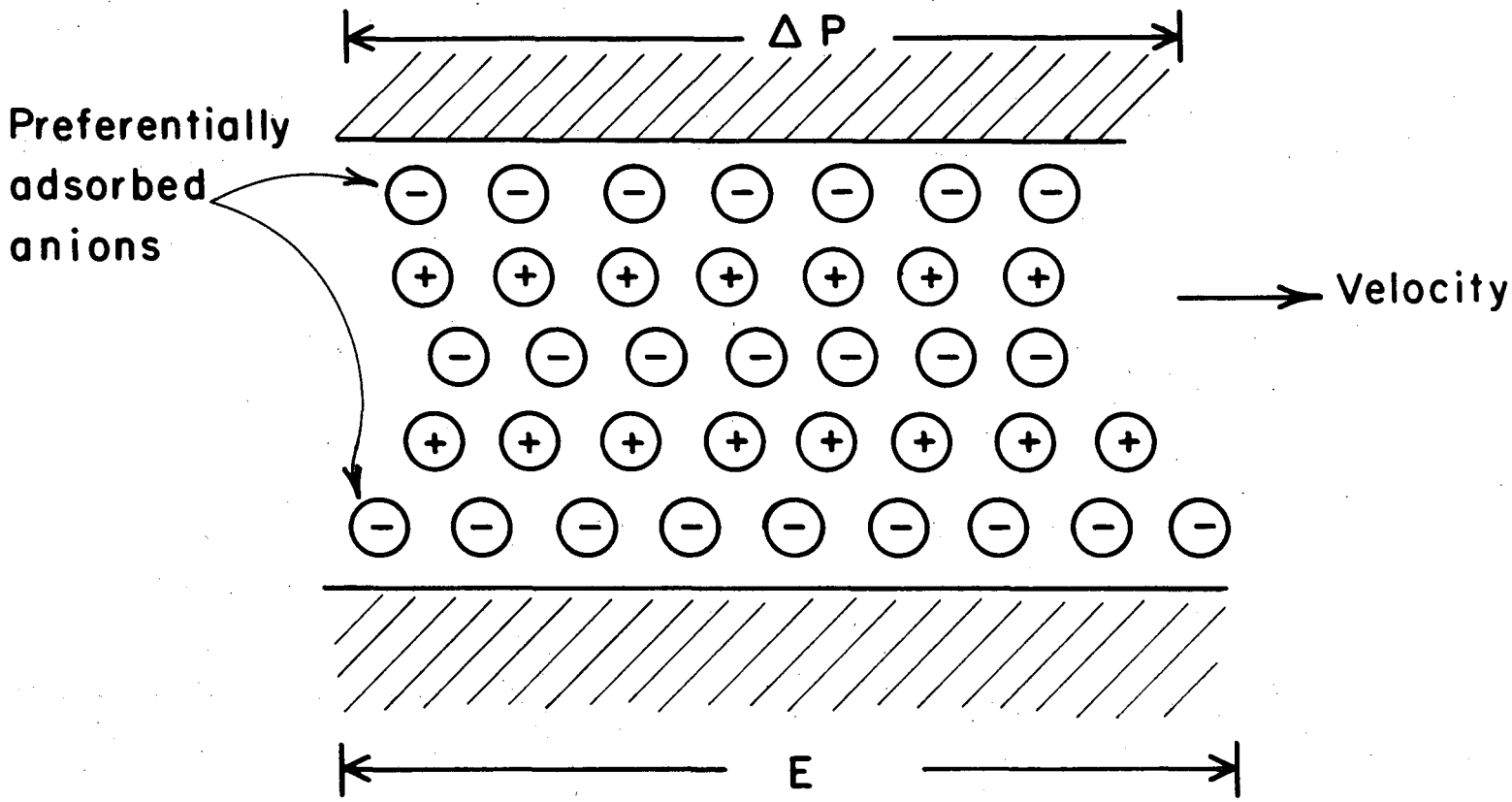

Fig. 3. Streaming Potential Model

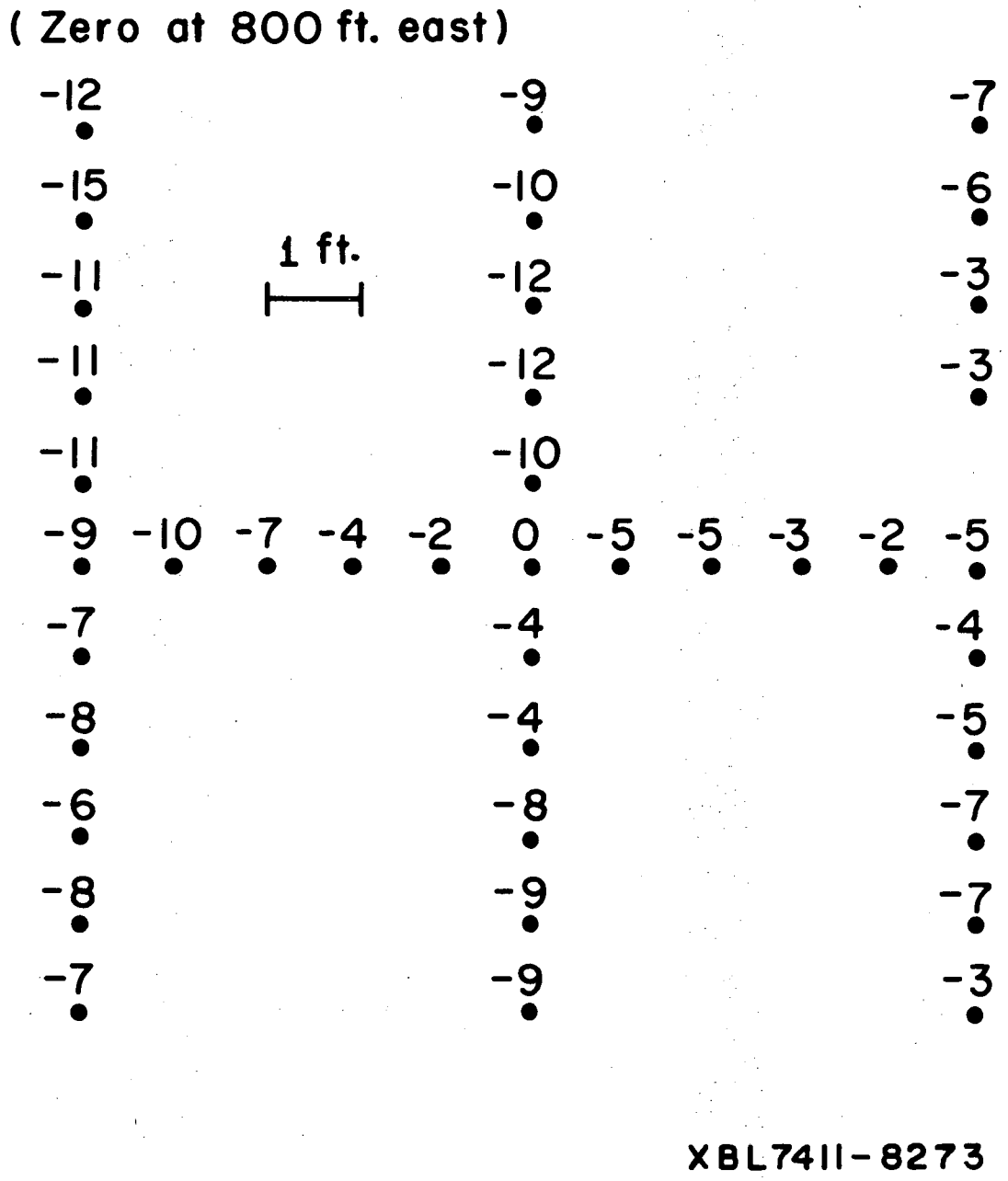

Fig. 4. Small-Scale Self-Potential Survey: Livermore Ranch, California.

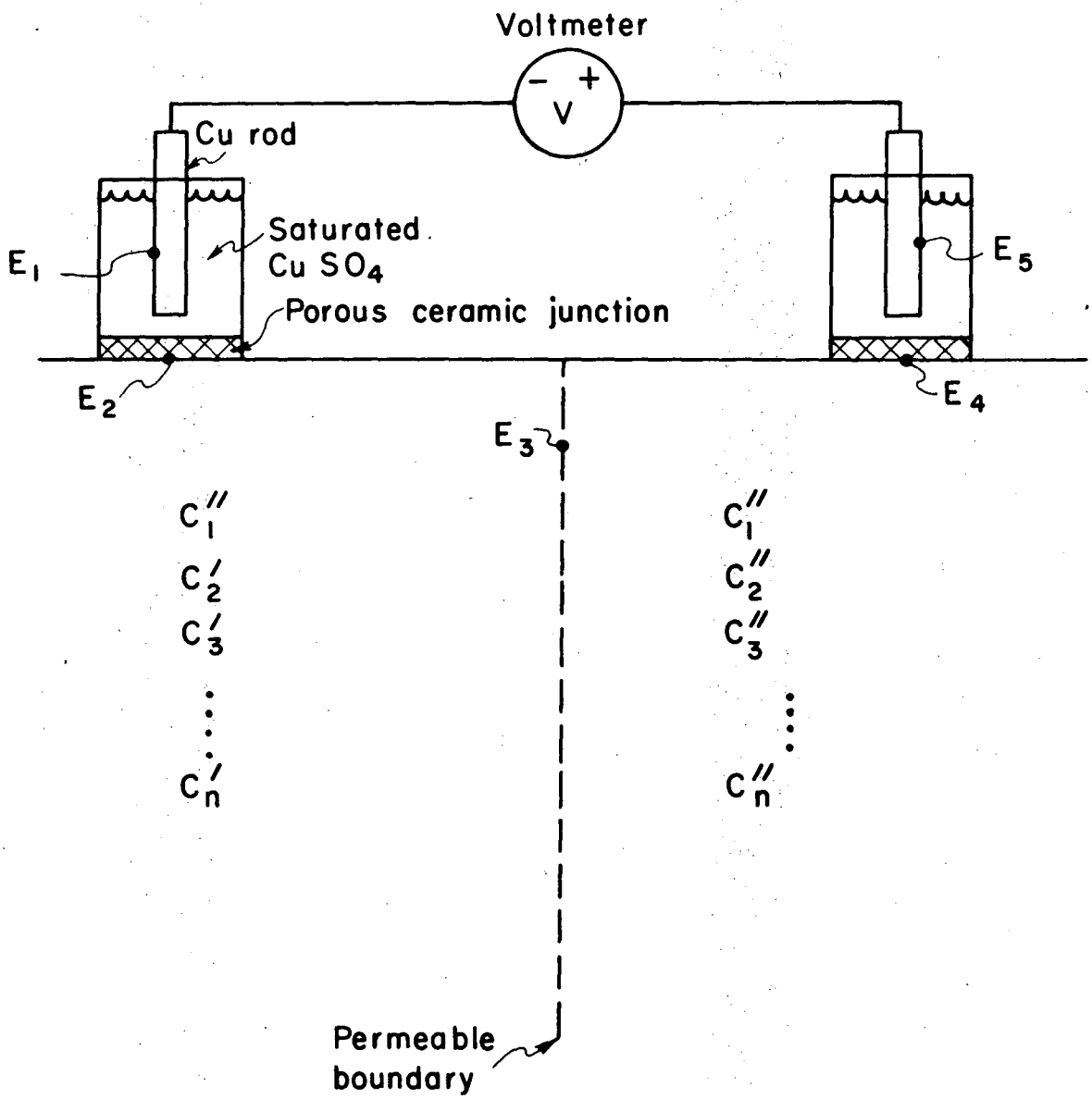

Fig. 5. Generation of Chemical Potentials.

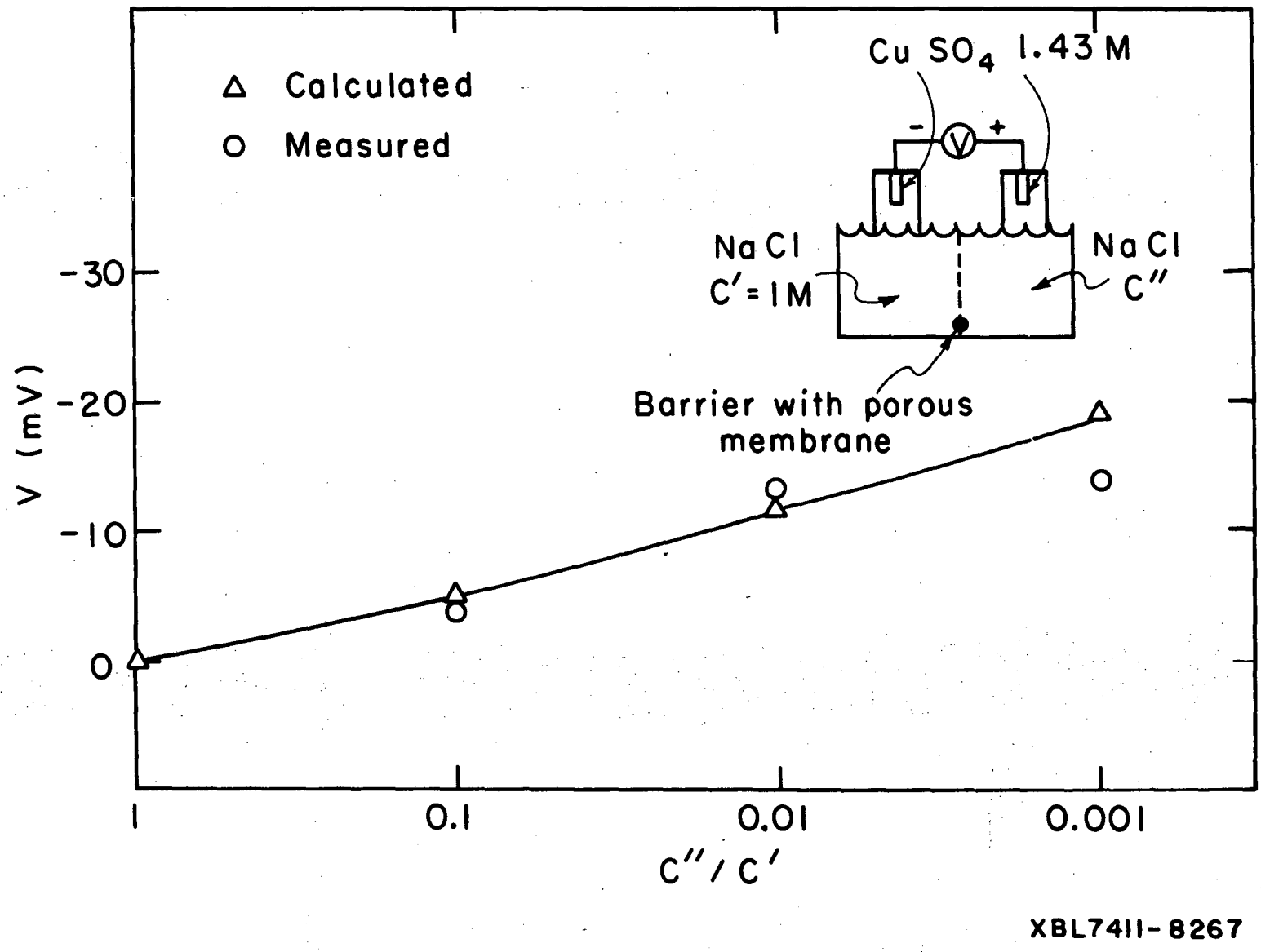

Fig. 6. Potential Between Cu-$CuSO_4$ Electrodes vs Concentration Change.

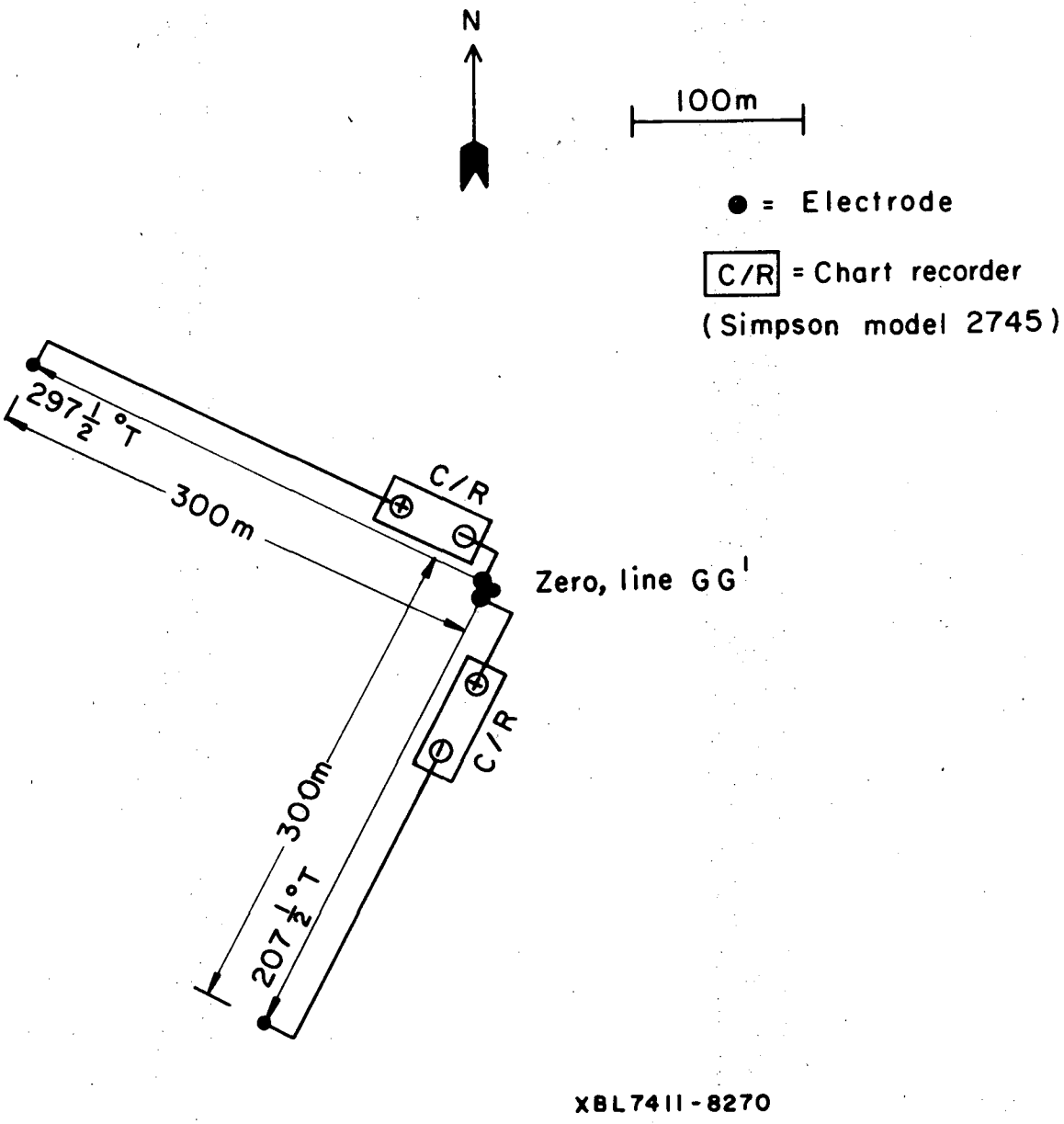

Fig. 7. Telluric Monitoring Dipole.

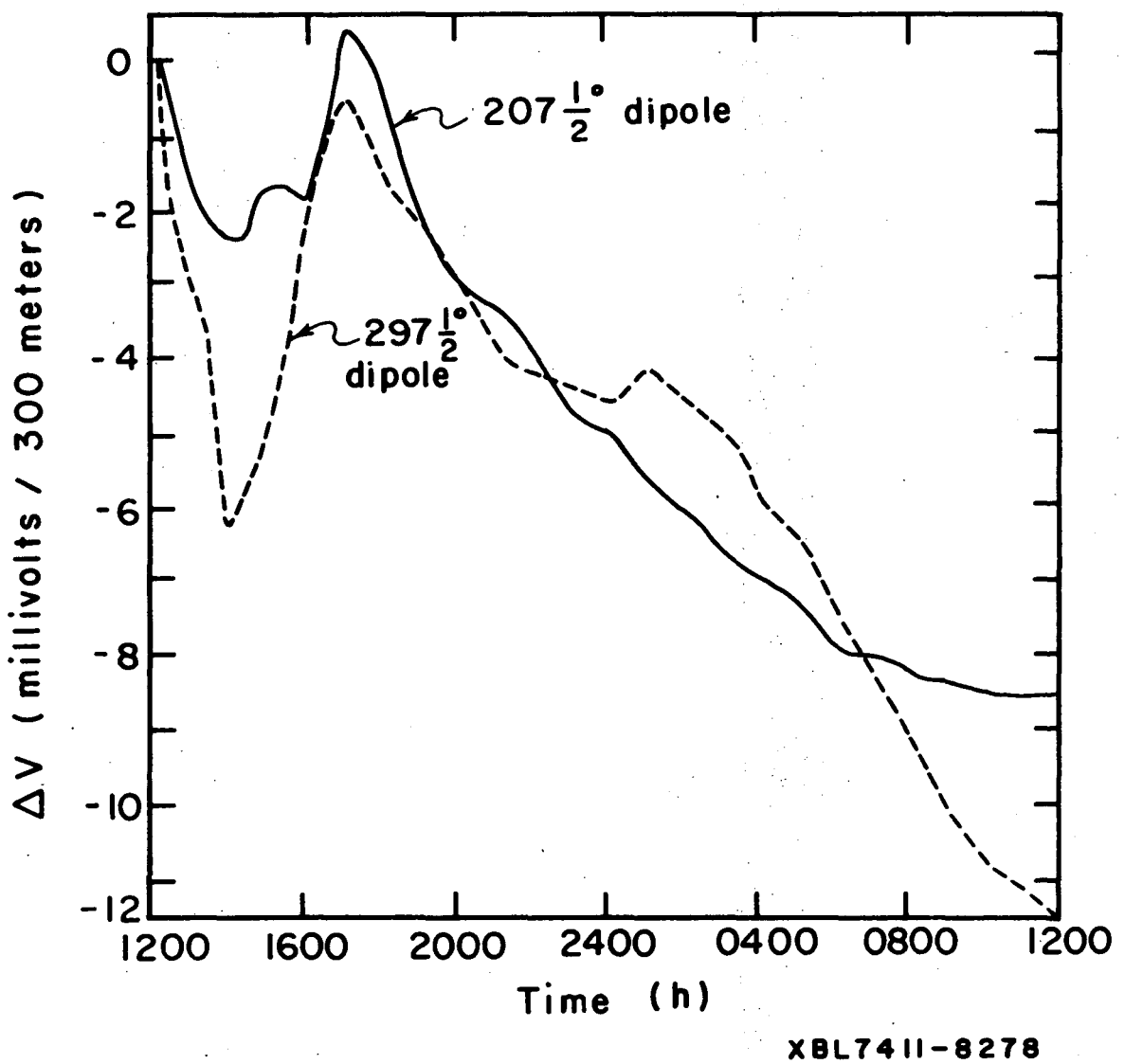

Fig. 8. Results of 24-Hour Telluric Monitoring.

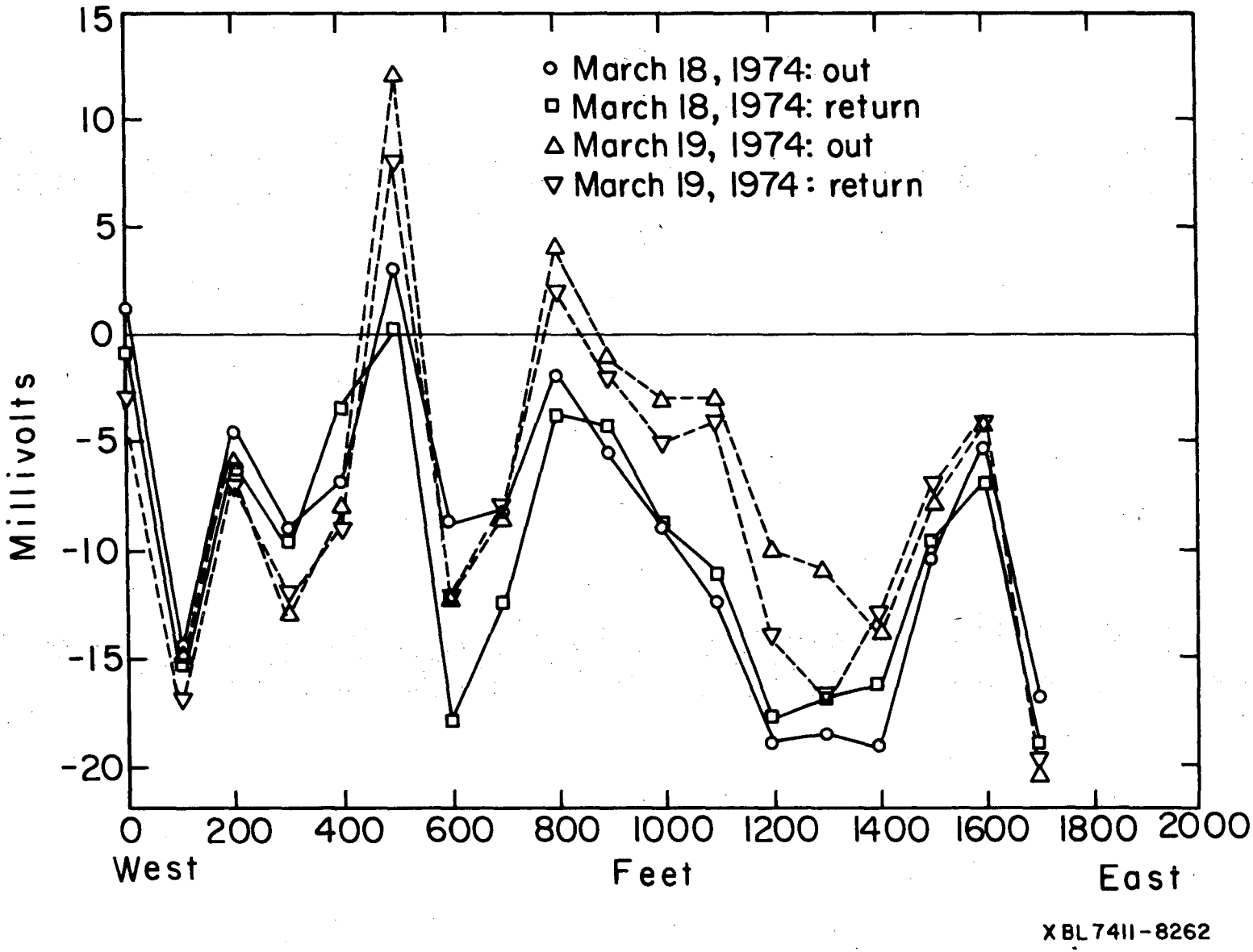

Fig, 9. Results of Repeated Surveys - Livermore Ranch, California.

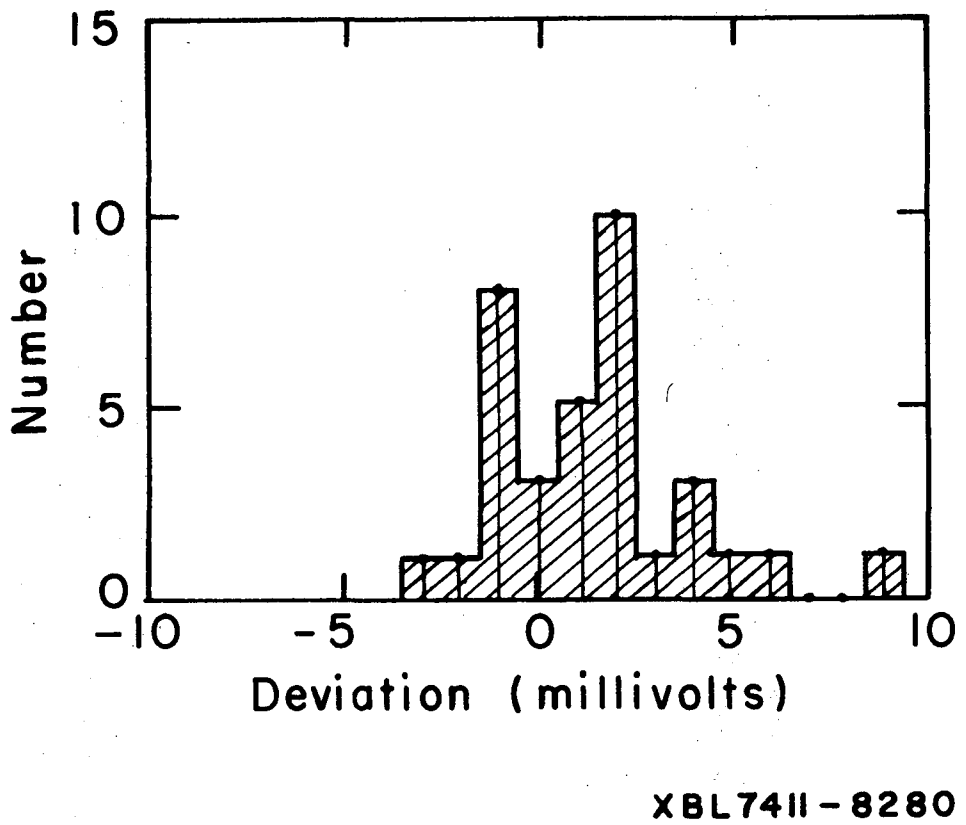

Fig. 10. Frequency Histogram of Reading Error.

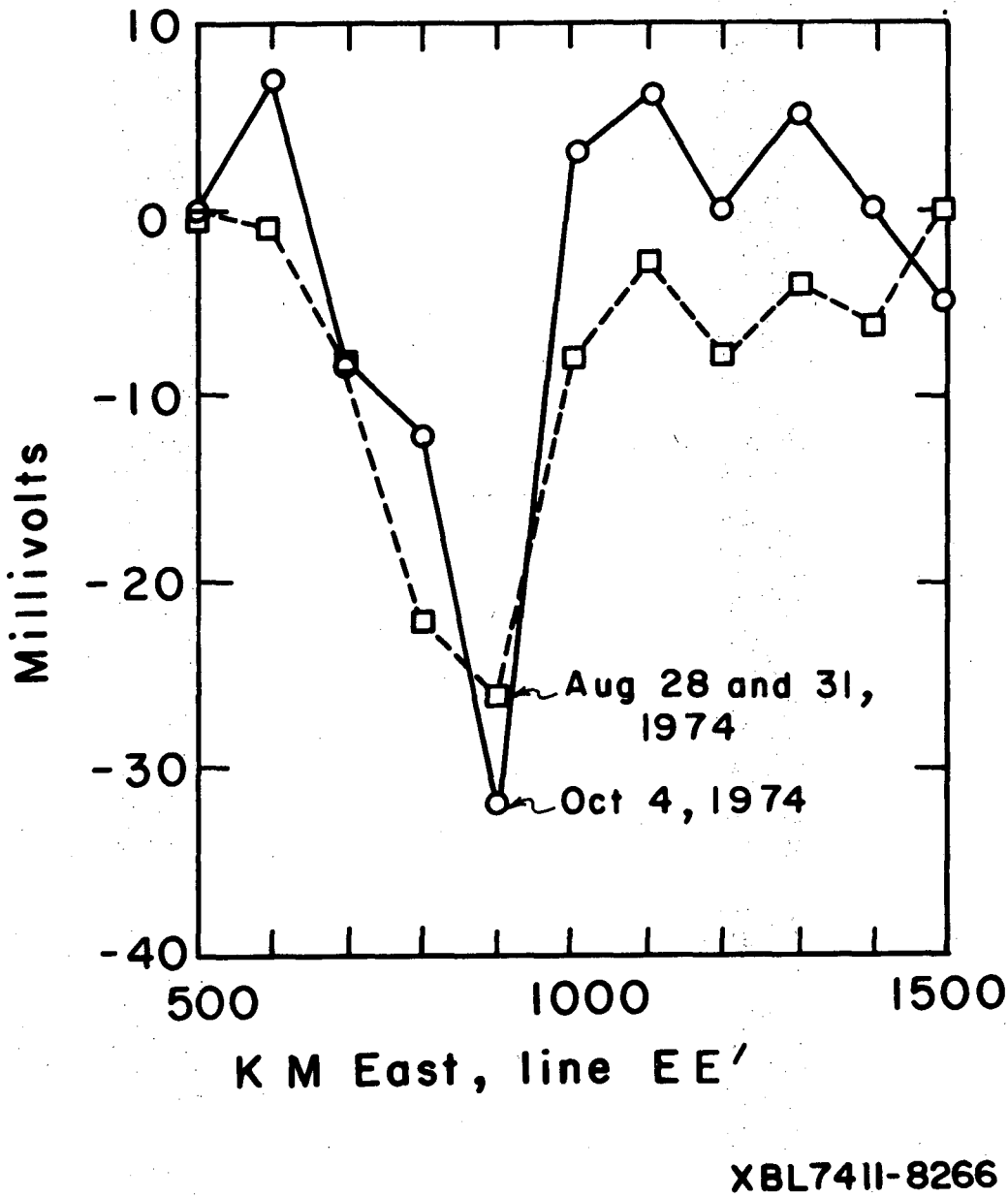

Fig. 11. Results of Repeated Surveys - Nevada Desert.

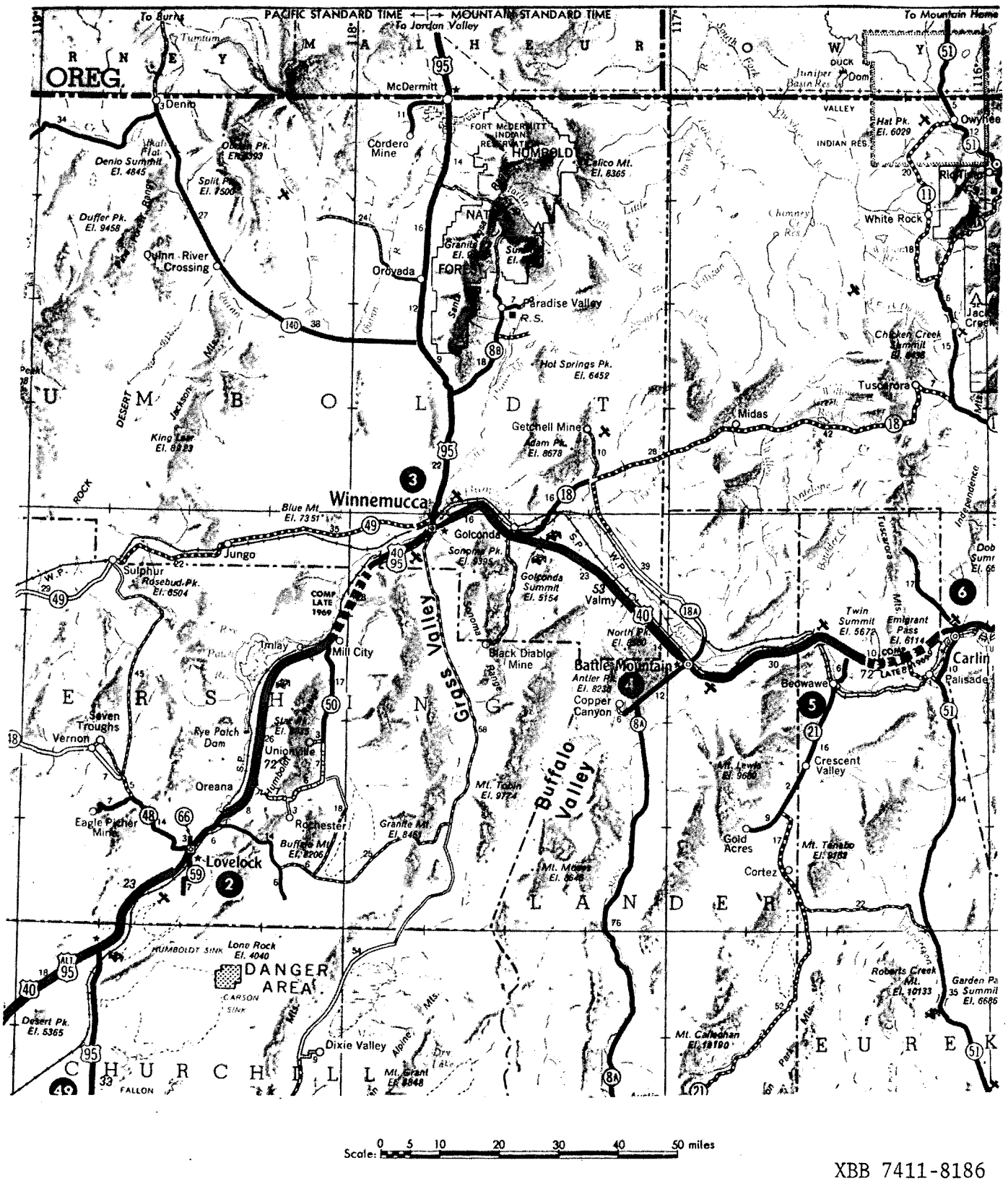

XBB 7411-8186

Fig. 12. Location Map of Neveda Survey Areas.

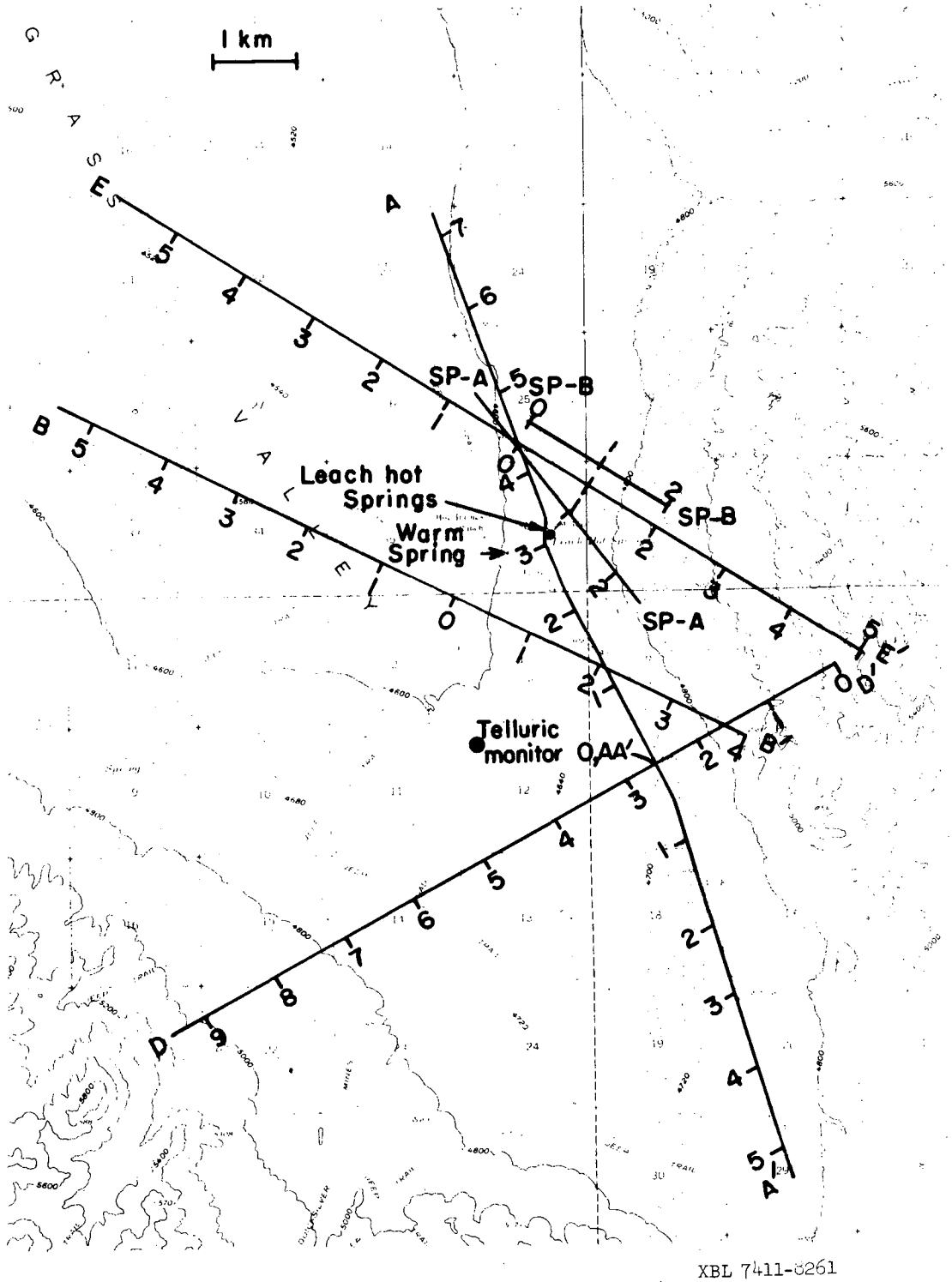

Fig. 13

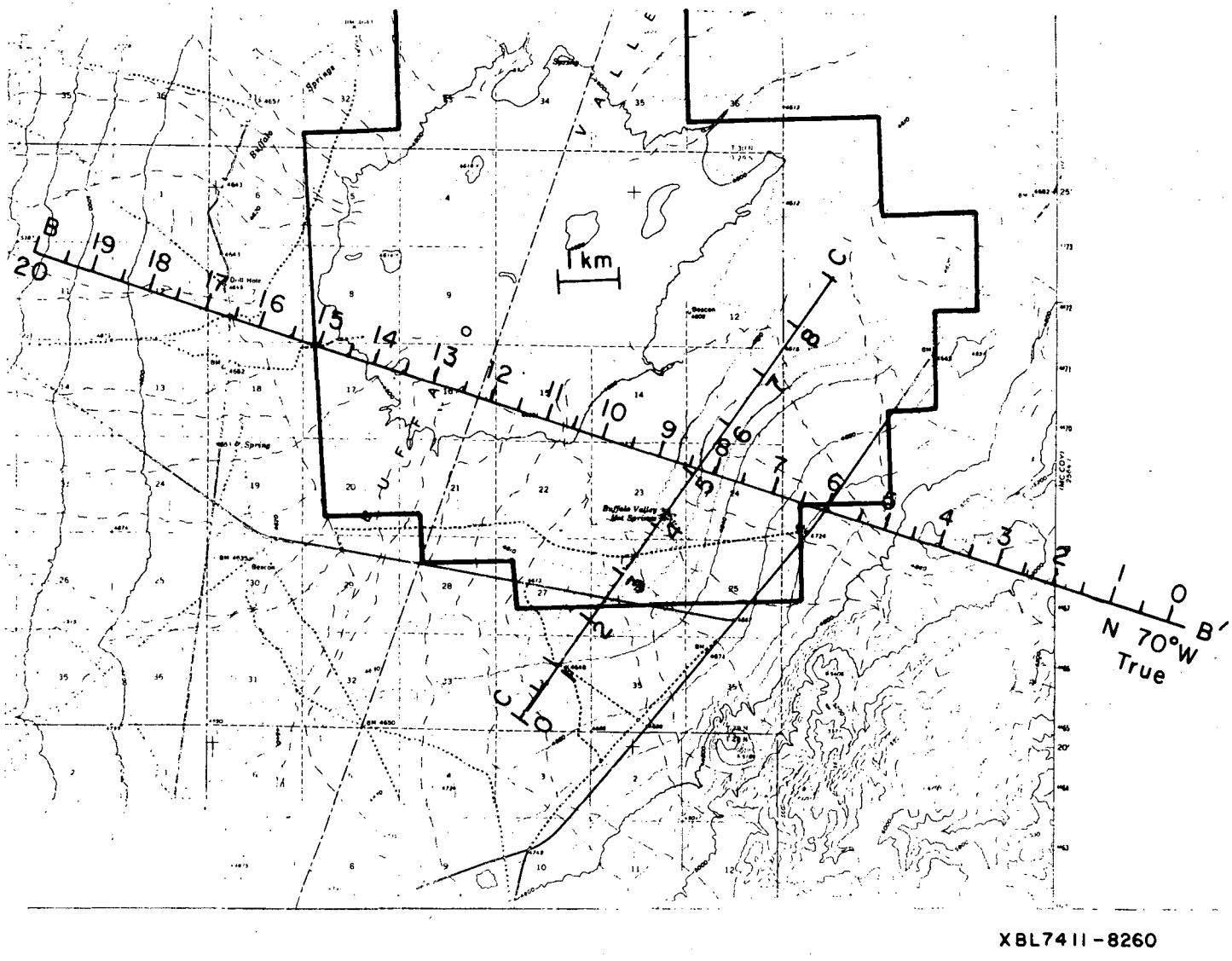

XBL7411-8260

Fig. 14. Survey Lines, Buffalo Valley, Nevada.

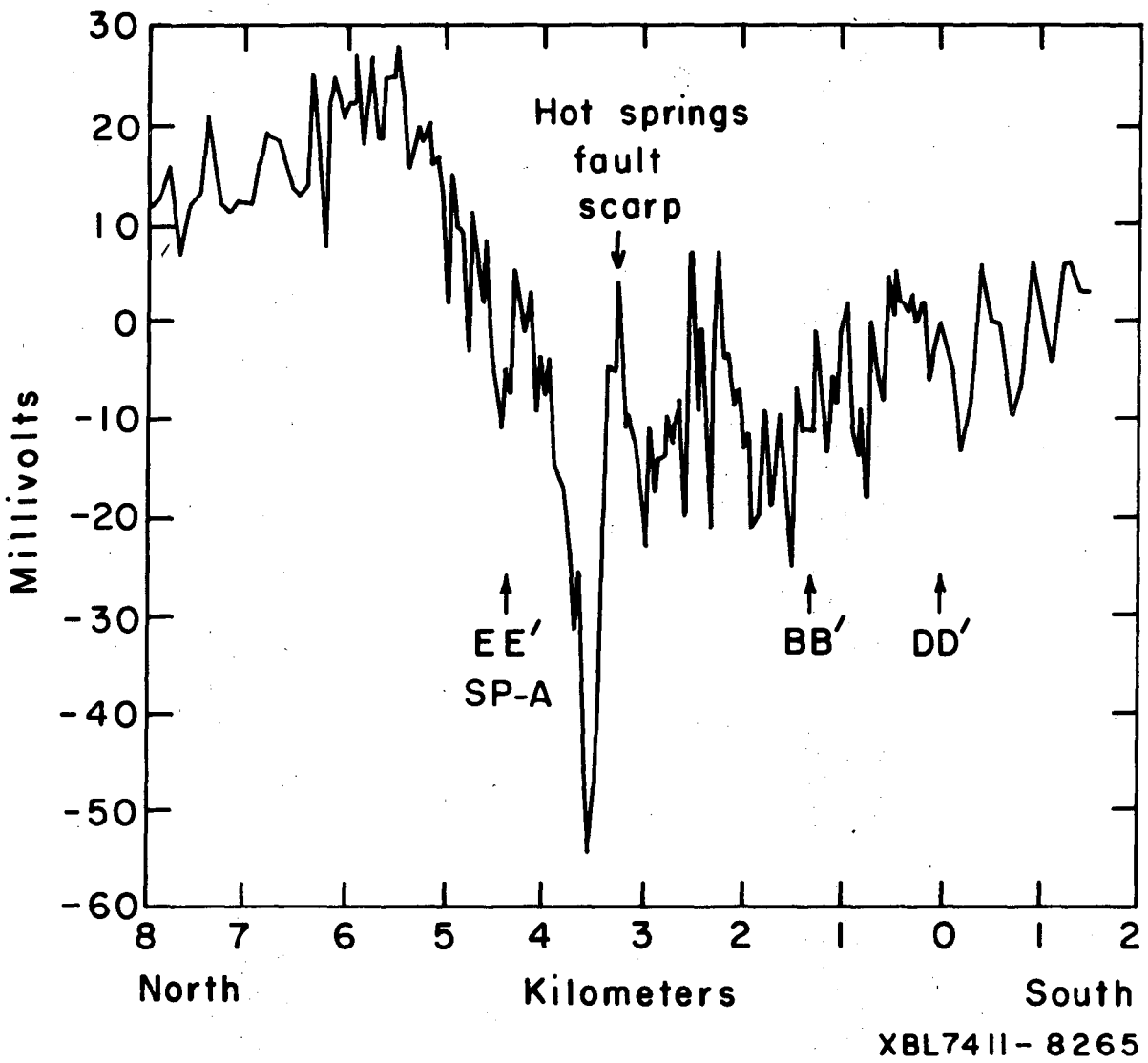

Fig. 15. Self-Potential Data, Line AA', Grass Valley.

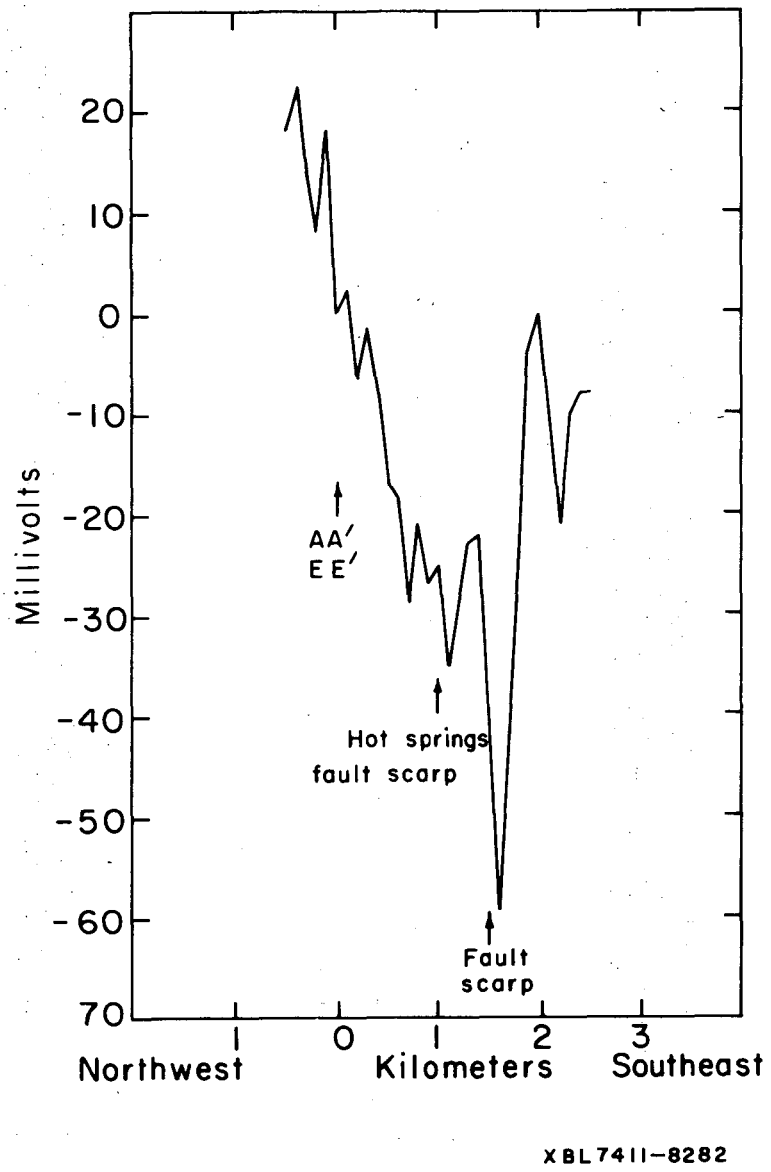

Fig. 16. Self-Potential Data, Line SP-A, Grass Valley.

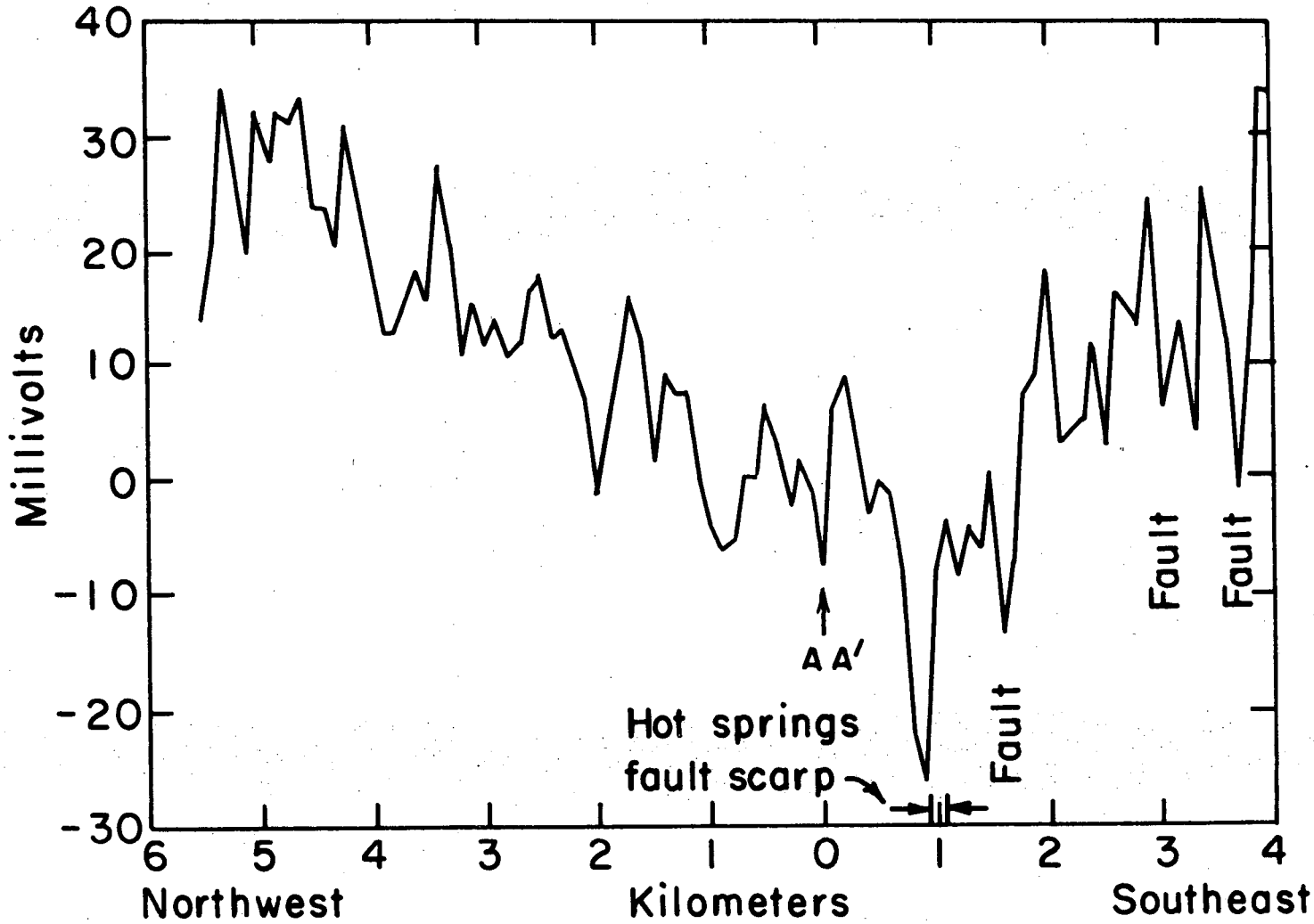

Fig. 17. Self-Potential Data, Line EE', Grass Valley.

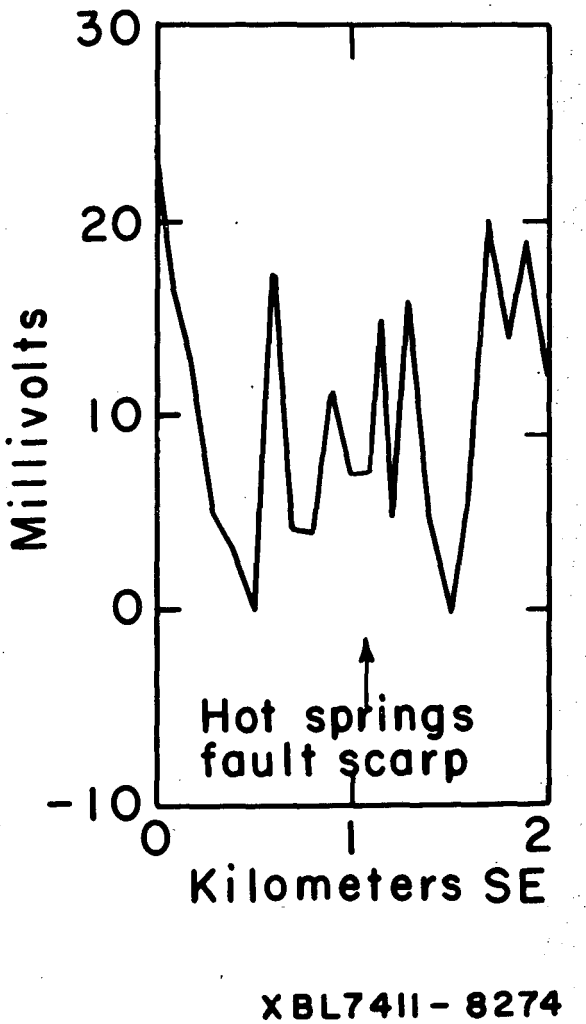

Fig. 18. Self-Potential Data, Line SP-B, Grass Valley.

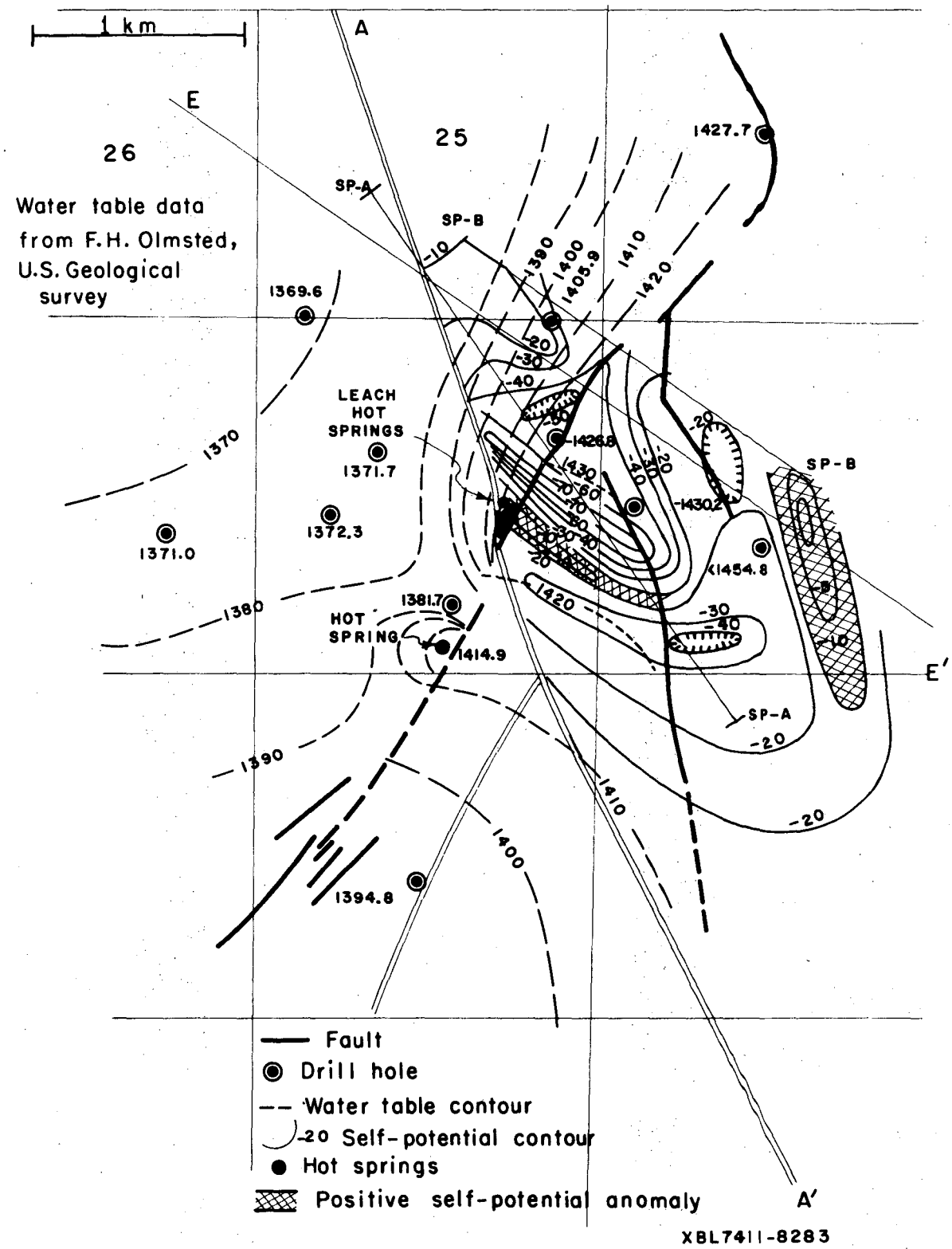

Fig. 19. Self-Potential and Water Table Contours, Leach Hot Springs Area, Grass Valley.

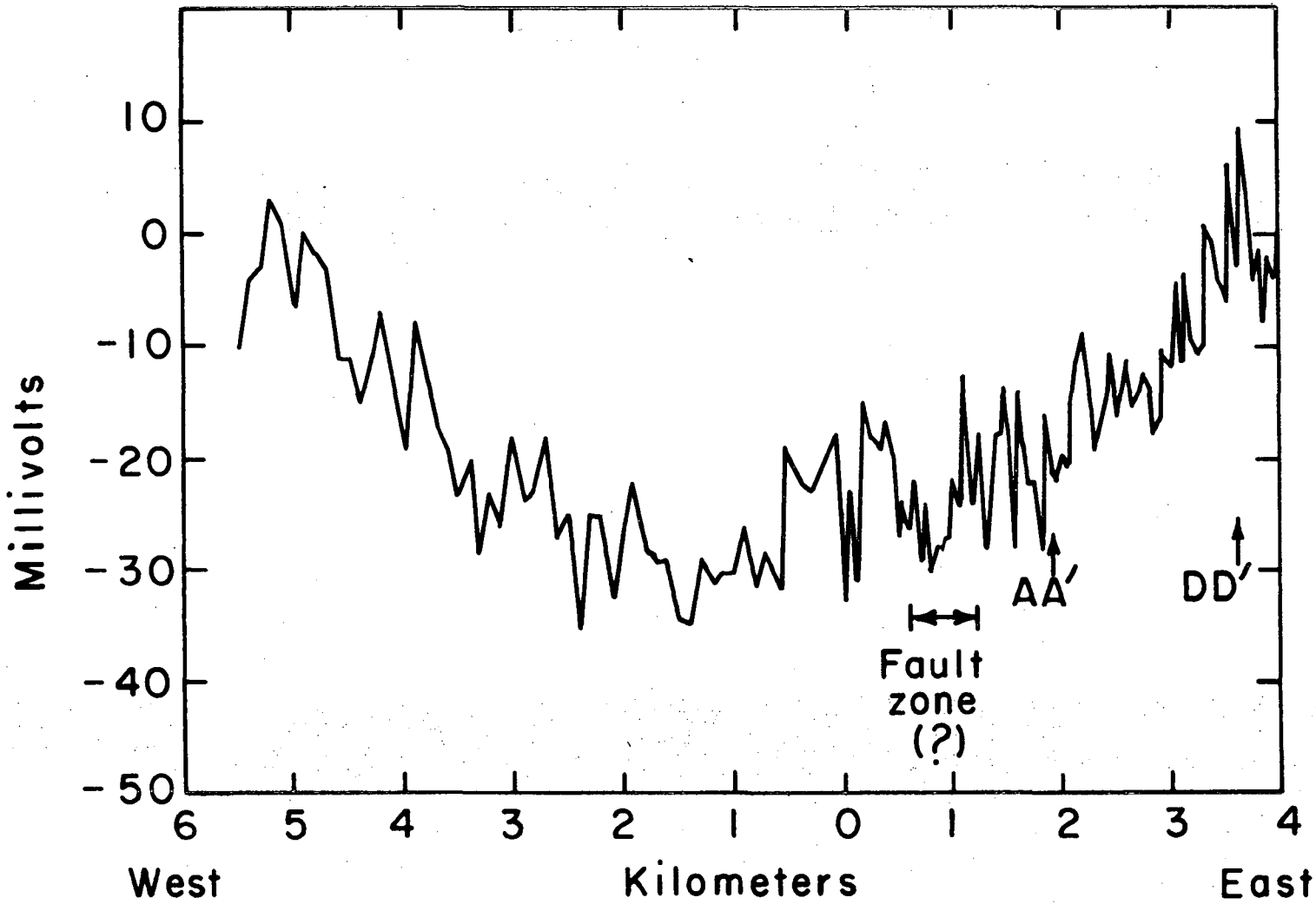

XBL7411-8263

Fig. 20. Self-Potential Data, Line BB', Grass Valley

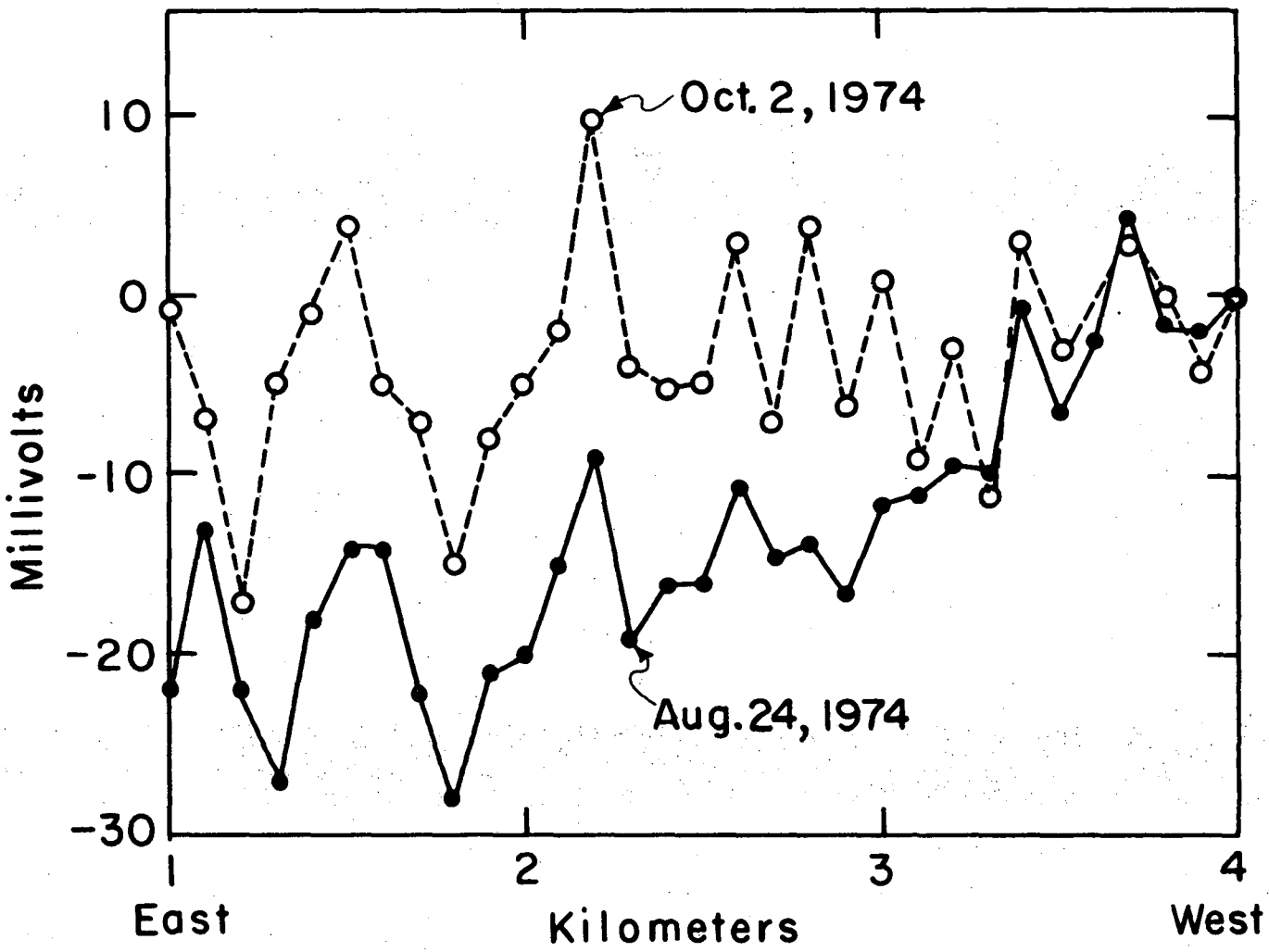

XBL7411-8275

Fig. 21. Re-run of Line BB', Grass Valley.

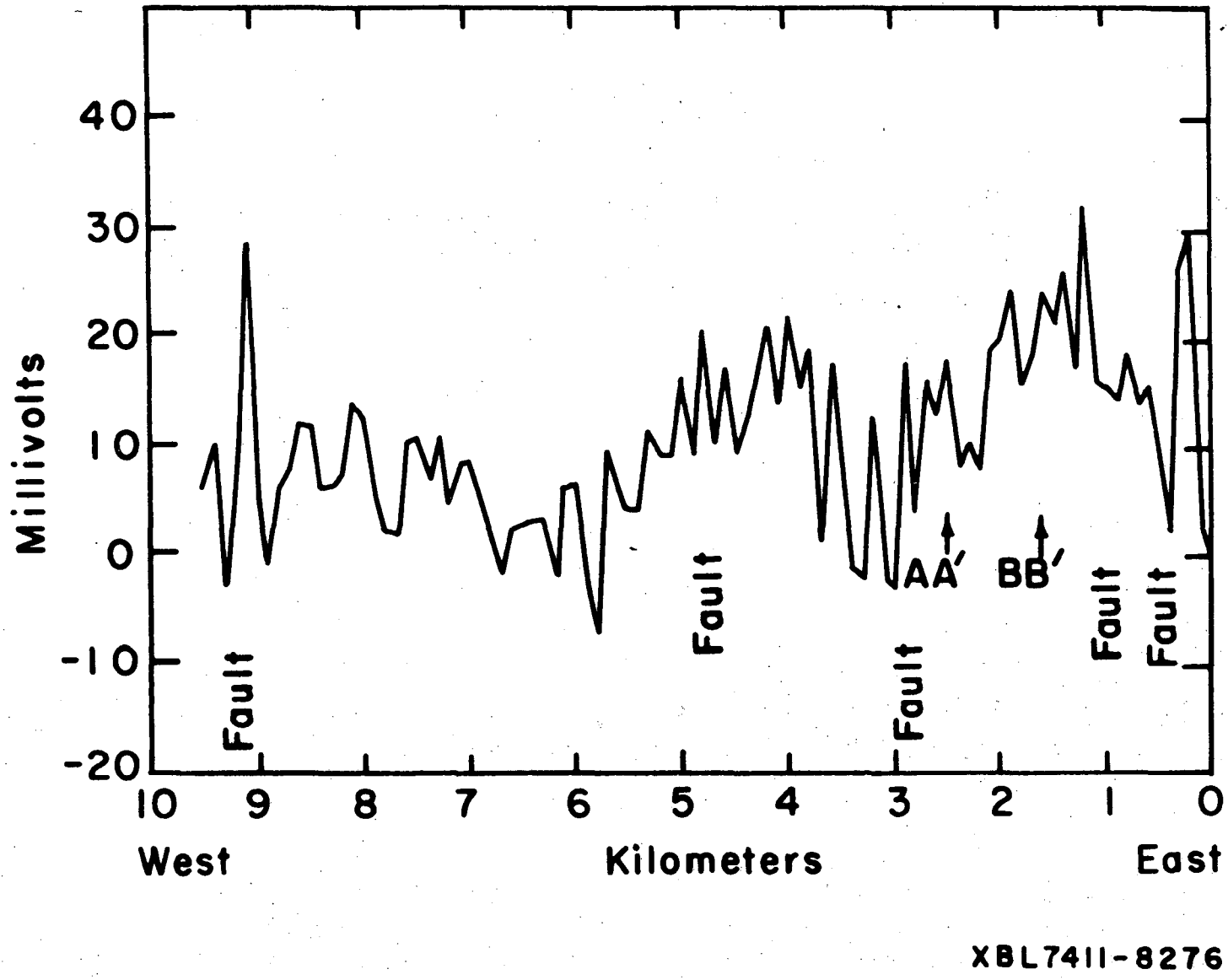

Fig. 22. Self-Potential Data, Line DD', Grass Valley.

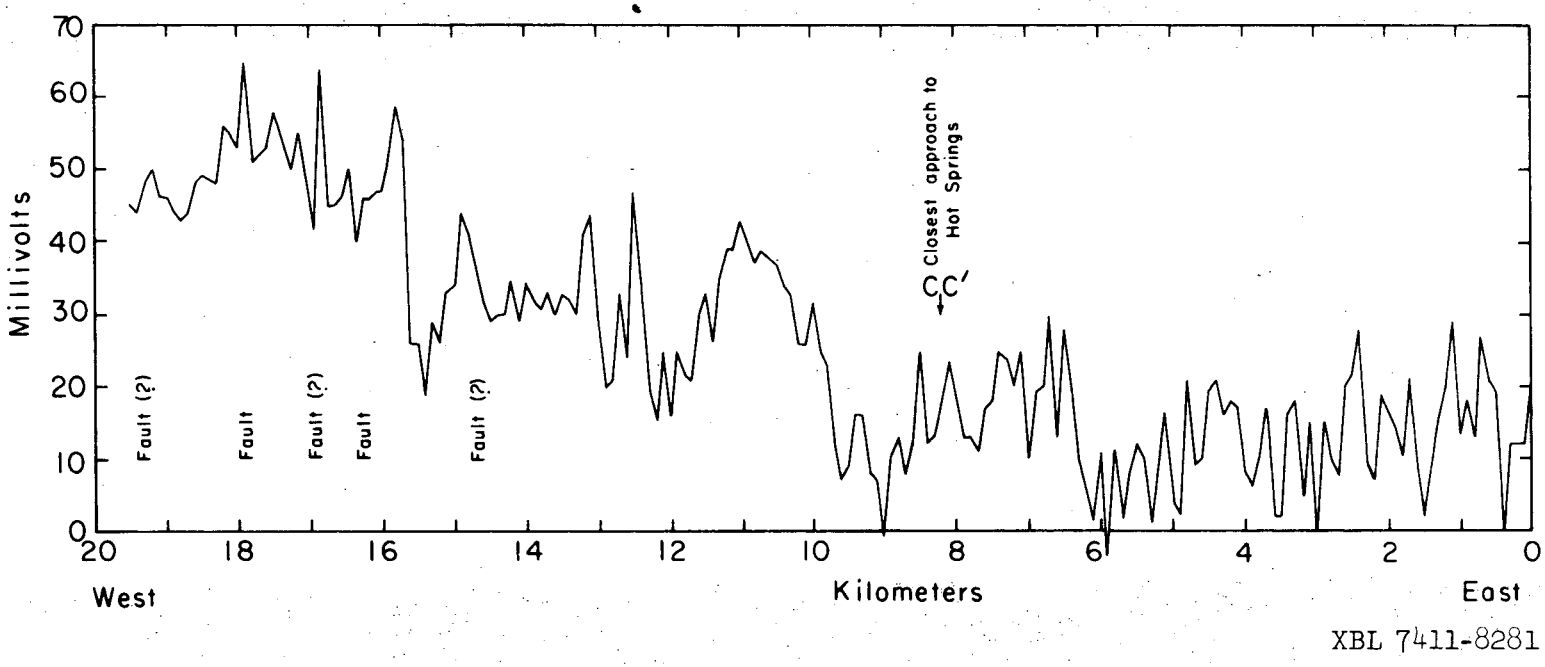

Fig. 23. Self-Potential Data, Line BB', Buffalo Valley.

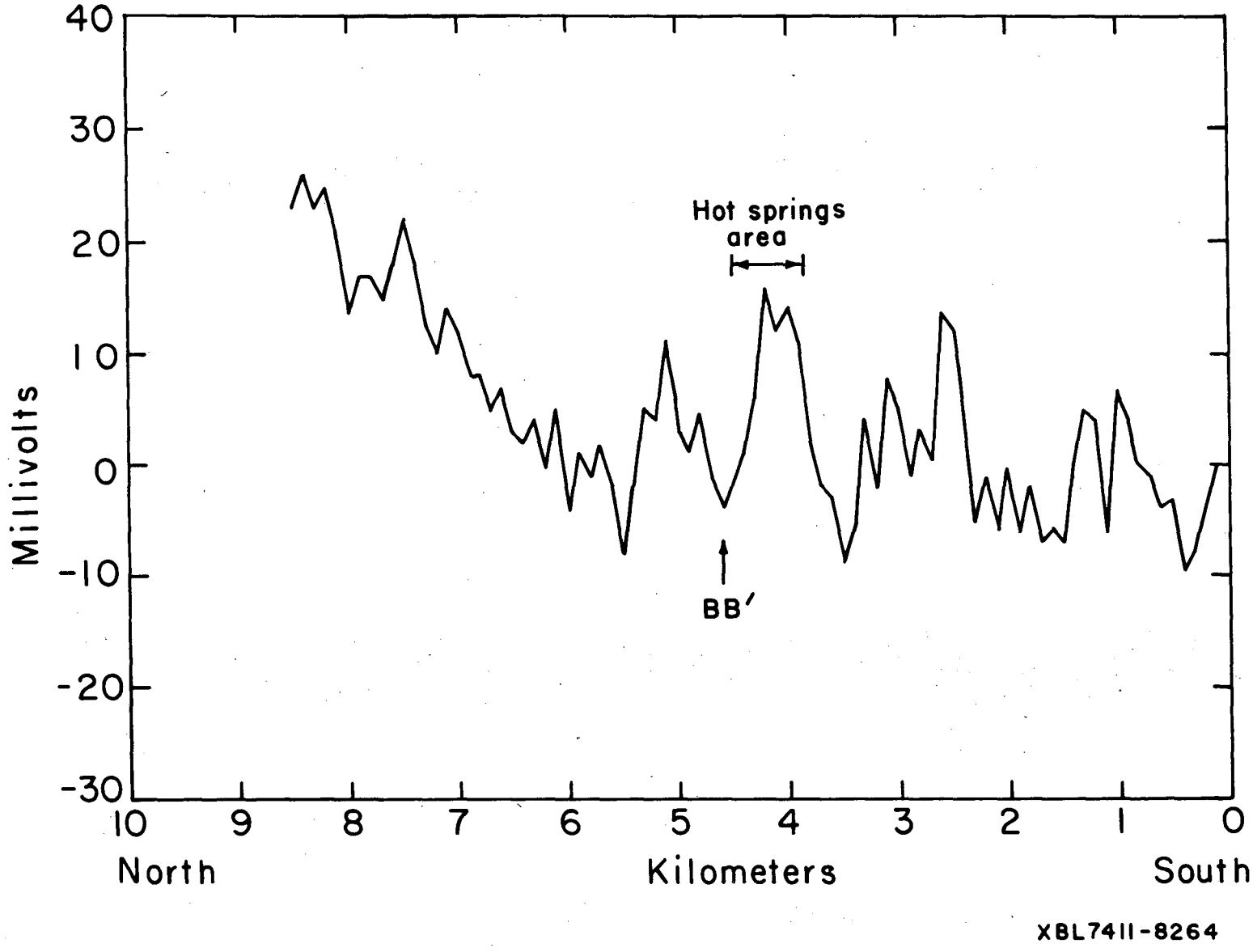

Fig. 24. Self-Potential Data, Line CC', Buffalo Valley.

TECHNICAL INFORMATION DIVISION
LAWRENCE BERKELEY LABORATORY
UNIVERSITY OF CALIFORNIA
BERKELEY, CALIFORNIA 94720